1982

Aerodynamics of closely coupled wings for varying chords and airfoil planforms

Gary D. Vincent

Department:

AERODYNAMICS OF CLOSELY COUPLED WINGS FOR VARYING CHORDS AND AIRFOIL PLANFORMS

BY

GARY D. VINCENT, 1959-

Presented to the Faculty of the Graduate School of the

UNIVERSITY OF MISSOURI-ROLLA

In Partial Fulfillment of the Requirements for the Degree

MASTER OF SCIENCE

IN

AEROSPACE ENGINEERING

1982

Approved by

Bruce P Selberg (Advisor) Walter Eckson

Troy L Hicks

PUBLICATION THESIS OPTION

This thesis has been prepared in the form of a paper for publication. Pages ix and 1 through 49 have been prepared for possible publication in the Journal of Aircraft of the American Institute of Aeronautics and Astronautics.

ABSTRACT

Aerodynamic characteristics of a dual wing aircraft were analyzed with variations in airfoil sections and chord ratios over existing equal chord ratio dual wing and monoplane aircraft designs. Two- and three-dimensional aerodynamic studies were conducted to find the wing geometry which would create the minimum cruise drag. The two-dimensional aerodynamic data was obtained from a multi-element inviscid vortex panel program coupled to a momentum integral boundary layer program to account for the aerodynamic coupling between the wings. With this data, a three-dimensional vortex lattice program calculated the three-dimensional aerodynamic data. Compared to an equal chord ratio dual wing aircraft, lower drag was found for the unequal chord ratio dual wing aircraft. This resulted from the two-dimensional aerodynamic data of the latter. In addition, these dual wing designs obtained superior performance compared to the equivalent monoplane.

TABLE OF CONTENTS

LIST OF ILLUSTRATIONS

LIST OF ILLUSTRATIONS (Continued)

LIST OF ILLUSTRATIONS (Continued)

LIST OF TABLES

FIGURE TITLES

AERODYNAMICS OF CLOSELY COUPLED WINGS FOR VARYING CHORDS AND AIRFOIL PLANFORMS

Gary D. Vincent*

Bruce P. Selberg+

University of Missouri-Rolla

---

*Graduate Student, Mechanical and Aerospace Engineering Department

+Professor of Aerospace Engineering, Mechanical and Aerospace Engineering Department, Member AIAA

ABSTRACT

Aerodynamic characteristics of a dual wing aircraft were analyzed with variations in airfoil sections and chord ratios over existing equal chord ratio dual wing and monoplane aircraft designs. Two- and three-dimensional aerodynamic studies were conducted to find the wing geometry which would create the minimum cruise drag. The two-dimensional aerodynamic data was obtained from a multi-element inviscid vortex panel program coupled to a momentum integral boundary layer program to account for the aerodynamic coupling between the wings. With this data, a three-dimensional vortex lattice program calculated the three-dimensional aerodynamic data. Compared to an equal chord ratio dual wing aircraft, lower drag was found for the unequal chord ratio dual wing aircraft. This resulted from the two-dimensional aerodynamic data of the latter. In addition, these dual wing designs obtained superior performance compared to the equivalent monoplane.

NOMENCLATURE

S	= stagger (in chord lengths)
G	= gap (in chord lengths)
D	= decalage angle (degrees)
α	= wing angle of attack (degrees)
c	= wing chord
b	= wing span
S_{ref}	= wing reference area
AR	= aspect ratio, b^2/S
λ	= taper ratio, c_{tip}/c_{root}
R_c	= Reynolds number based upon wing chord
R	= Reynolds number per meter (foot)
C_p	= pressure coefficient, $(p - p_\infty)/q_\infty$
x/c	= nondimensional chordwise location
c_l	= sectional lift coefficient
C_L	= total lift coefficient
$C_{L_{cr}}$	= cruise lift coefficient
c_d	= sectional drag coefficient
C_D	= total drag coefficient
C_{D_i}	= induced drag coefficient
$C_{D_{cr}}$	= cruise drag coefficient
$C_{u/l}$	= upper to lower airfoil chord ratio
c_l/c_d	= sectional lift-to-drag ratio
L/D	= total lift-to-drag ratio
$(L/D)_{cr}$	= cruise lift-to-drag ratio
C_{l_α}	= sectional lift curve slope

V_{cr} = cruise speed

P_{cr} = cruise power

D_{cr} = cruise drag

W_{cr} = cruise weight

I. INTRODUCTION

At the dawn of aviation history the biplane and triplane configurations were used to enhance the structural integrity of the airplane's lifting surfaces. By using improved structural framework monoplane designs replaced these multiplane configurations. Also, propulsion systems became lighter and more powerful enabling aircraft to fly faster and requiring smaller wing areas, hence eliminating the need for multiplane systems altogether. However, recent studies of a dual wing system have shown it to have lower drag than its single wing counterpart, defined as a single wing producing the same lift as the dual wing.

Four terms of current use in the study of a dual airfoil system are stagger, S, gap, G, decalage, D, and chord ratio, $C_{u/l}$. Both stagger, the longitudinal separation of the airfoils, and gap, the vertical distance between the airfoils, are measured from mid-chord to mid-chord and nondimensionalized with respect to the lower airfoil chord, c_l, illustrated in Figure 1. Gap is always positive; stagger is positive when the upper airfoil is ahead of the lower airfoil. Positive decalage occurs when the upper airfoil is at a higher angle of incidence than the lower airfoil. Chord ratio is defined as the ratio of the upper airfoil chord to the lower airfoil chord.

The earliest record of an aerodynamic investigation into the performance of biplanes occurred in 1918 when Norton (1) conducted a limited number of three-dimensional wind tunnel tests on non-symmetric airfoils. These tests were performed at a constant G=1, and D=0°. Stagger was varied from S=+1 to S=-1 in 0.25 increments. Essentially three conclusions were made. First, S=+1 produced the highest

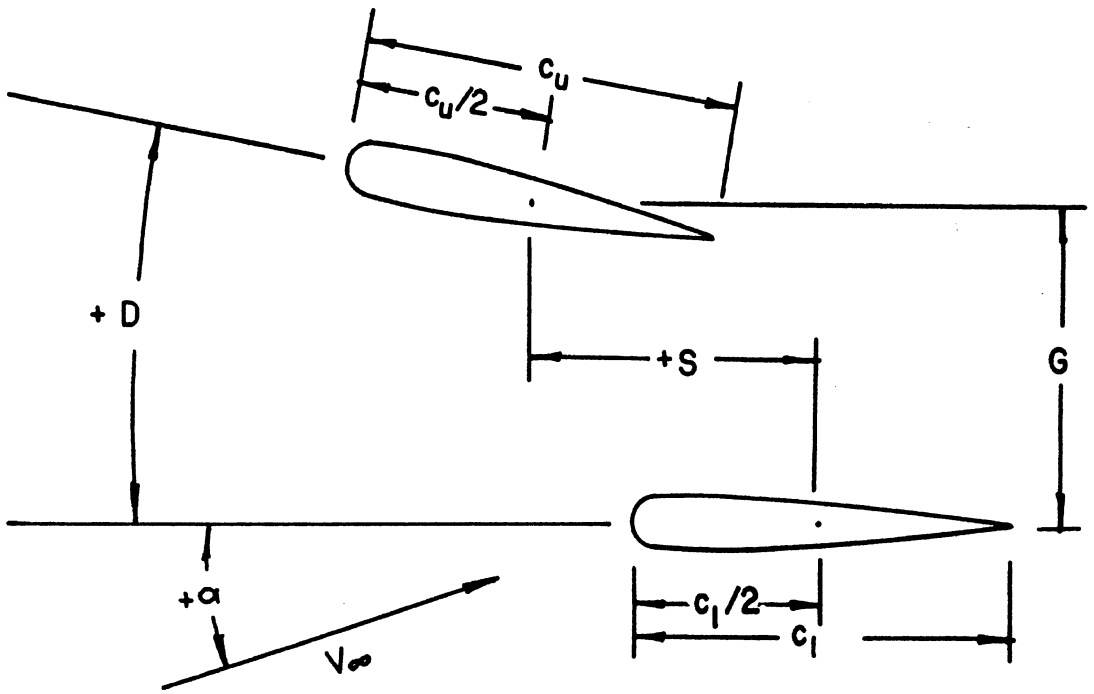

NOTE: S and G are nondimensionalized with respect to c_l

Figure 1. Dual Wing Geometric Relationships

performance for the range tested. Second, the center of pressure flucuated very little for this wing system. Finally, the relative properties of the individual airfoils contributed little to the performance of the dual configuration.

Knight and Noyes (2,3,4) in 1929 repeated Norton's stagger studies while performing a gap and decalage analysis. Their research revealed that by decreasing the proximity of the wings, with large staggers or gaps, or both, the loads on each wing became similar, reflecting the aerodynamic decoupling of the wings. Also, the maximum lift coefficient decreased for all nonzero decalages.

In 1934 Prandtl and Tietjens (5) developed analytical procedures which led to their discovery of two-dimensional induced drag of biplanes. They concluded this phenomenon resulted in some dual wing configurations having lower induced drag than an equivalent single wing.

Conformal mapping was used by Garrick (6), in 1935, to analytically determine the pressure distribution over dual airfoils. Two NACA 4412 airfoils at S=1, G=1, and D=0° were mapped into a plane where analytical data was extracted.

By 1936, Nenadovitch (7) performed the first two-dimensional systematic series of tests on a dual airfoil system compared to a single airfoil producing the same lift as the dual airfoil system. Results from these test indicated S=1, G=0.33, and D=-6° gave the least drag with respect to an equivalent monoplane. All three values occurred at the extreme ends of the testing range.

Three-dimensional wind tunnel tests were performed by Olson and Selberg (8) in 1974. Dual and single wings of equal lift capacity

were tested. From these tests, it was shown that drag coefficients were lower for some dual wing configurations in comparison with an equivalent single wing. This resulted in the dual wing obtaining a higher lift to drag ratio than the single wing.

In the same year, Smith (9), in an effort to obtain higher maximum lift coefficients, discussed analytical results of investigations of multi-component airfoils, including dual airfoil configurations. However, no investigation was aimed at optimizing for the minimum drag system. Hence, these facts contributed little to the goal of maximizing cruise performance of dual airfoil systems.

Rokhsaz and Selberg (10), in 1980, using the NACA 0012 and NACA 63_2-215 airfoils, performed an analytical investigation of dual airfoil configurations in comparison to their single airfoil counterparts. The results of Rokhsaz and Selberg indicated that a dual airfoil system could reduce the two-dimensional drag by 13% or more over the single airfoil. Also, the mechanism for the drag reduction was extensively investigated.

In the following year, Rhodes (11) applied the analytical methods of Reference (10) to two state-of-the-art airfoils, MS(1)-0313 and NL(S)-0715F. Dual wing studies for both airfoils where the same airfoil was used for upper and lower wing indicated that S=1, G=0.26, and D=-6° gave less drag than their single wing counterparts. Two dual wing aircraft, a six- and a twelve-place, were designed using the two-dimensional results for both airfoils. In comparison with their single wing baseline aircraft, the MS(1)-0313 dual wing aircraft achieved 4-10% more range; likewise, the NL(S)-0715F dual wing version obtained 4% more range.

None of the above researchers varied the airfoils or the chord ratios relative to one another in their dual wing studies. Therefore, the first phase of the present study is intended to find the dual airfoil configuration that attains the largest sectional lift-to-drag ratio improvement over the single airfoil, through chord ratio and airfoil variation. Four state-of-the-art airfoils will be used, MS(1)-0313, NL(S)-0715F, RONCZ 1073 and 1085 (12). During the second and final phase of this study, two dual wing aircraft will be designed using the dual airfoil results of the first phase. The performance of these aircraft will be compared against a "baseline" aircraft and against a dual wing aircraft of equal chords and of like airfoils.

As illustrated in Figure 2, the MS(1)-0313 airfoil is a 13% thick turbulent flow airfoil, a modified version of the LS(1)-0413 (GA(W)-2) airfoil. The NL(S)-0715F airfoil, a 15% thick laminar flow airfoil, is designed for $R_c = 9 \times 10^6$ at a cruise lift coefficient of 0.2. For cruise, the NL(S)-0715F airfoil deflects a 20% chord simple flap upward ten degrees. Concerning the RONCZ airfoils, no airfoil shapes can be published at this time, as requested by the author (12).

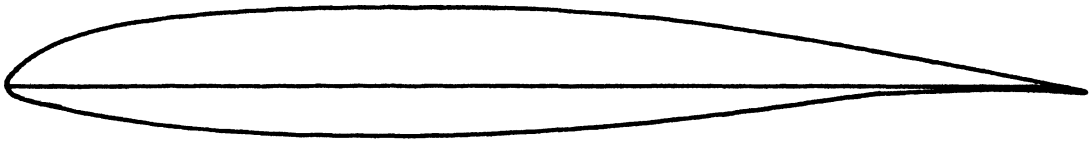

MS(1)-0313 Airfoil Shape

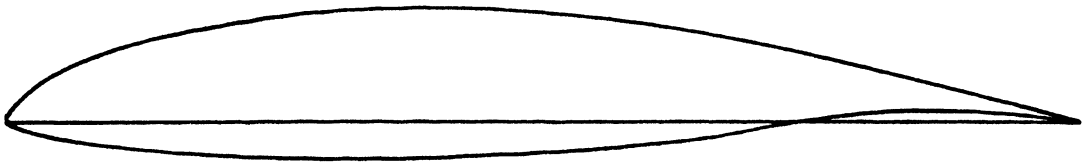

NL(S)-0715F Airfoil Shape

Figure 2. MS(1)-0313 and NL(S)-0715F Airfoil Shapes

II. DUAL WING TRADE OFF STUDIES

To analytically determine the optimum combination of stagger, decalage, chord ratio, and airfoil sections, a detailed parametric study was conducted on the following airfoils: MS(1)-0313, NL(S)-0715F, RONCZ 1085, and RONCZ 1073. The results of Rhodes (11) indicated the most favorable configuration was S=1, G=0.26, and D=-6° in two and three dimensions for both the MS(1)-0313 and the NL(S)-0715F airfoils. Starting at this dual wing position the two-dimensional viscous and three-dimensional induced drag results were minimized first through a selection of similar or disimiliar airfoils. Next, chord ratios were varied while holding the other three parameters constant. In this manner the configuration which results in the greatest improvement in the wing lift-to-drag ratio can be found.

This study implemented three programs developed by Rokhsaz and Selberg (10) which calculated the potential flow about dual airfoil sections using a distributed vortex panel approach. The first program generated the airfoil grid points, which were spaced for a specified velocity gradient. In the second program the principles of the vortex panel method were used to calculate the potential flow solution, assuming a linear vortex strength distribution over a polygon approximating the airfoil. The third program, using the data from the second program, estimated the boundary layer thickness and viscous drag.

The boundary layers were calculated by a momentum integral boundary layer technique. The momentum integral procedure used Thwaites' method (13) to predict the laminar flow solution. Location

of the laminar-turbulent transition point was determined by Michel's transition criterion (14). Once in the turbulent regime, Head's momentum integral method (15) was utilized. Viscous drag was calculated using the Squire-Young formula (16).

Results from the combined vortex panel viscous boundary layer program were compared to experimential results (17,18) at equivalent Reynolds numbers. Figure 3 illustrates the high degree of correlation between theory and experiment for the MS(1)-0313, at a $R_c=2.1x10^6$, and NL(S)-0715F, at a $R_c=3.0x10^6$. A Young's factor of 2.45 and 2.15 was used for the MS(1)-0313 and the NL(S)-0715F, respectively, in the Squire-Young equation. Comparable accuracy was obtained at other Reynolds numbers. Unfortunately, no experimental data was available for the RONCZ airfoils. Hence, only the relative effects of the dual wing over its single wing counterpart were discussed. Finally, the induced drag calculations were obtained from the vortex lattice program using inputs from the two-dimensional vortex panel program.

From Rhodes (11), the dual airfoil configuration that gave the largest sectional lift-to-drag ratio over the single airfoil occurred at S=1, G=0.26, and D=-6°. This optimum dual airfoil system was found for both the MS(1)-0313 and the NL(S)-0715F airfoil. With this dual airfoil placement as an initial starting position, Figures 4 through 15 graphically illustrate the details of the parametric study. The sectional lift-to-drag ratio is shown as a function of the sectional lift coefficient for several configurations of the airfoil sections investigated.

Results for the dual MS(1)-0313 airfoil section are shown in Figures 4 through 7. Figure 4 illustrates the chord ratio less than

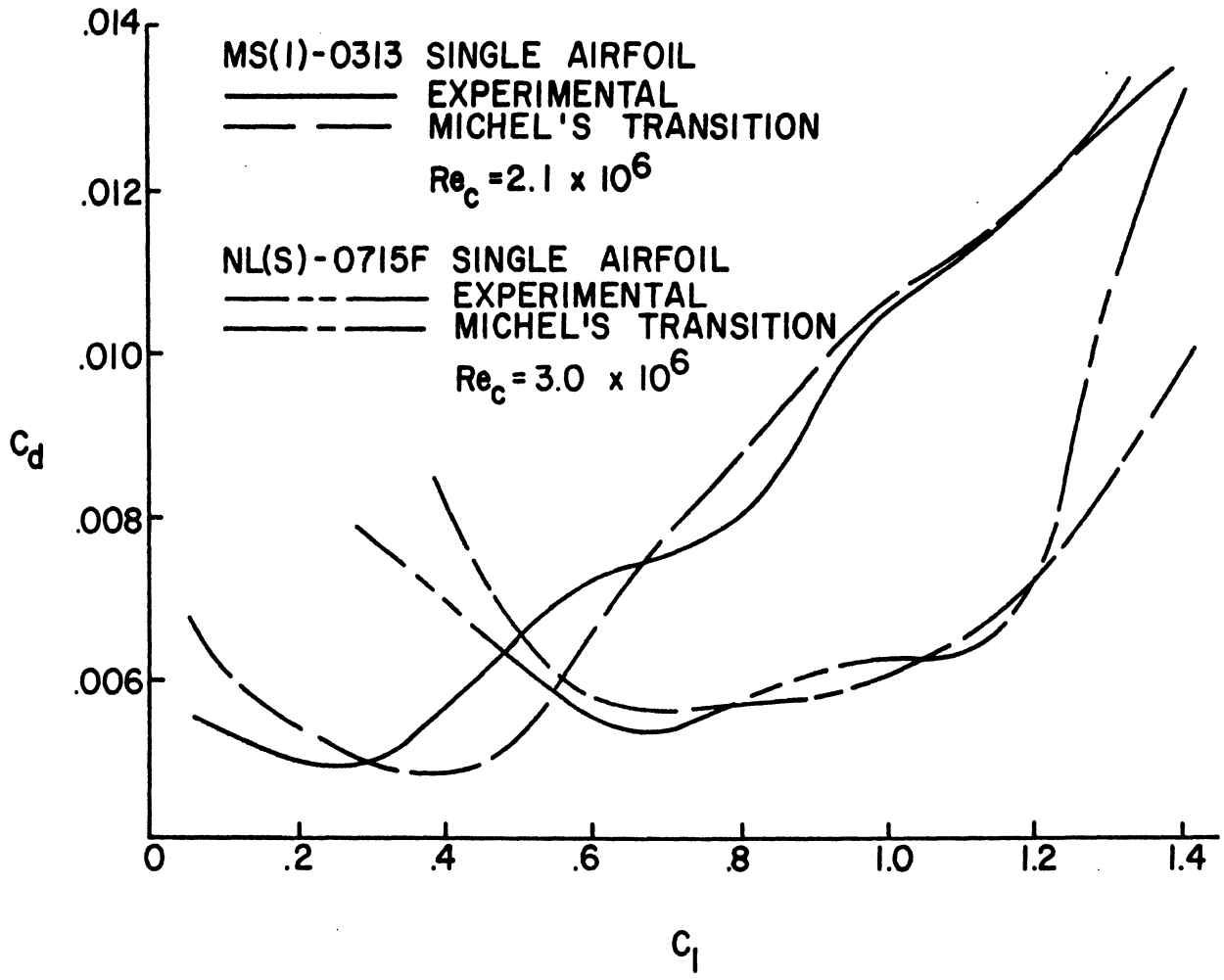

Figure 3. Comparison of Theoretical with Experimental Results

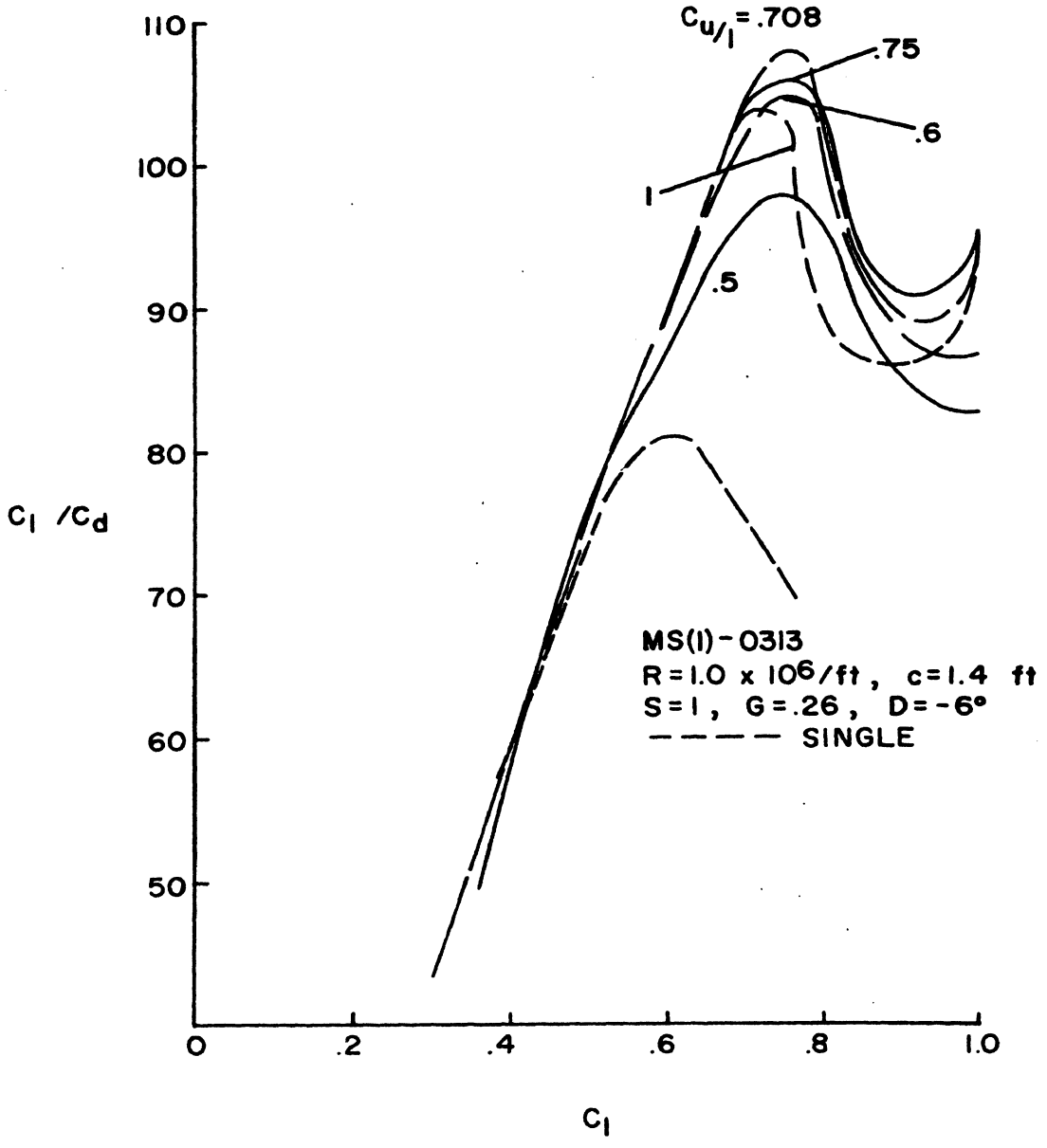

Figure 4. MS(1)-0313 Two-Dimensional Chord Ratio Less Than One Study Results

unity study for constant stagger, gap, and decalage. A chord ratio of 0.708 peaked beyond the other ratio cases. Variations above or below 0.708 resulted in reduced performance, that is higher two-dimensional drag for a given two-dimensional lift coefficient. For all these cases S=1, G=0.26, and D=-6° remained constant.

By using the chord ratio of 0.708, a stagger variation was performed to obtain the greatest sectional lift-to-drag ratio for the dual airfoil as compared to a single airfoil for a given lift coefficient, that is the optimum aerodynamic coupling for the dual airfoil. For constant values of gap, decalage, and chord ratio, S=1 gave the best two-dimensional results, and gave substantial gains over the single airfoil. Figure 5 shows these stagger results. Other values near S=1 fell below in performance. However, the S=1 values occurred at higher sectional lift coefficients.

The two-dimensional variable decalage analysis is summarized in Figure 6. By holding the other three parameters constant, decalage was varied above and below D=-6°. The maximum sectional lift-to-drag ratios for D=-7° and D=-8° peaked above the D=-6° case. However, the D=-7° and D=-8° cases were inferior to D=-6° at lower sectional lift coefficients. Also, the D=-8° results fell below the single airfoil for lift coefficients less than and equal to 0.5. In contrast to the equal chord configuration, the D=-6° was superior over the D=-7° case since the D=-7° fell below the equal chord ratio case shown by Figures 4 and 6.

Variations in gap between any of the airfoils were not performed since Rhodes (11) showed that optimum aerodynamic coupling occurred at G=0.26 for the equal chord study of both the MS(1)-0313 and

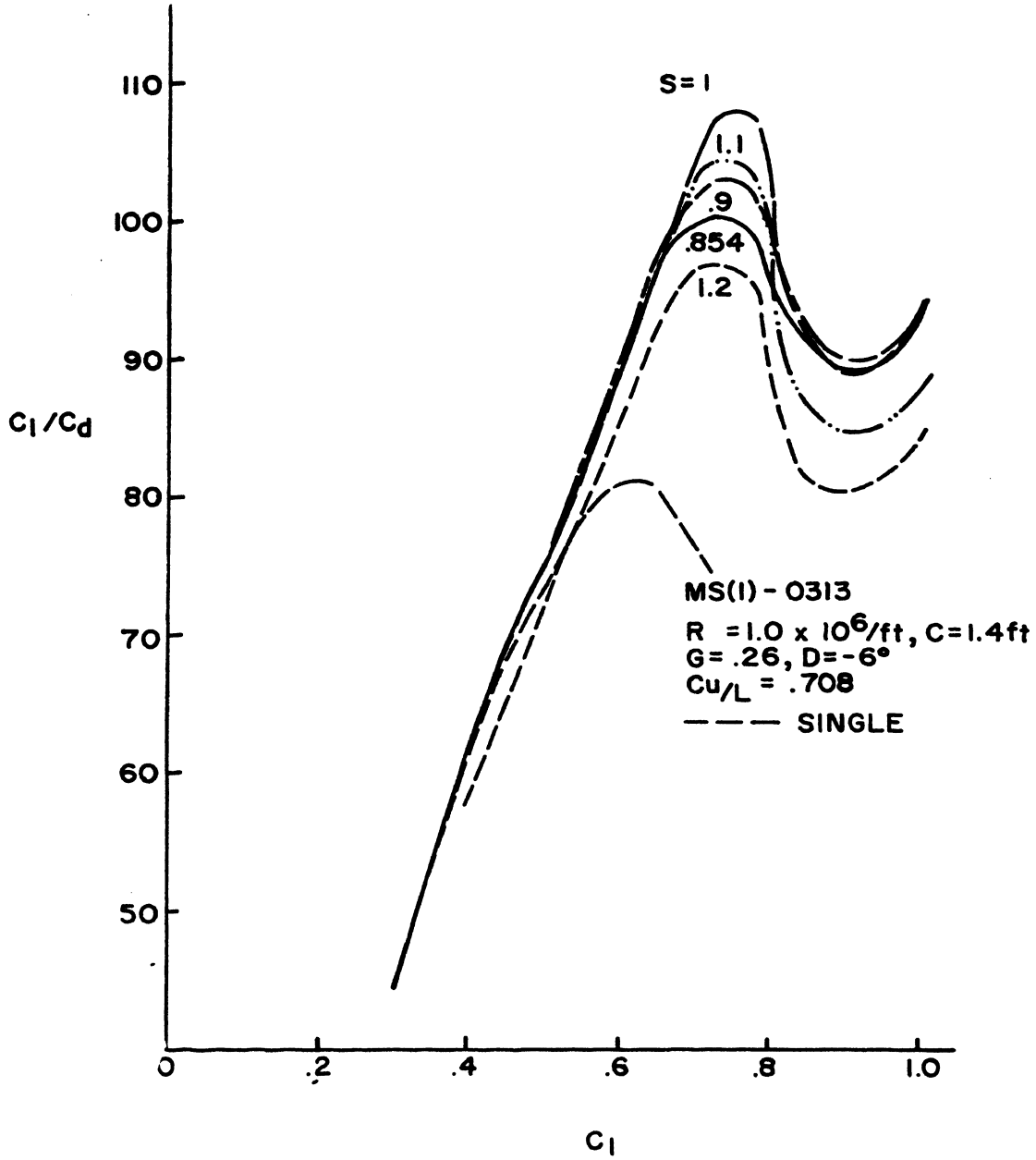

Figure 5. MS(1)-0313 Two-Dimensional Stagger Study Results for Chord Ratio Less Than One

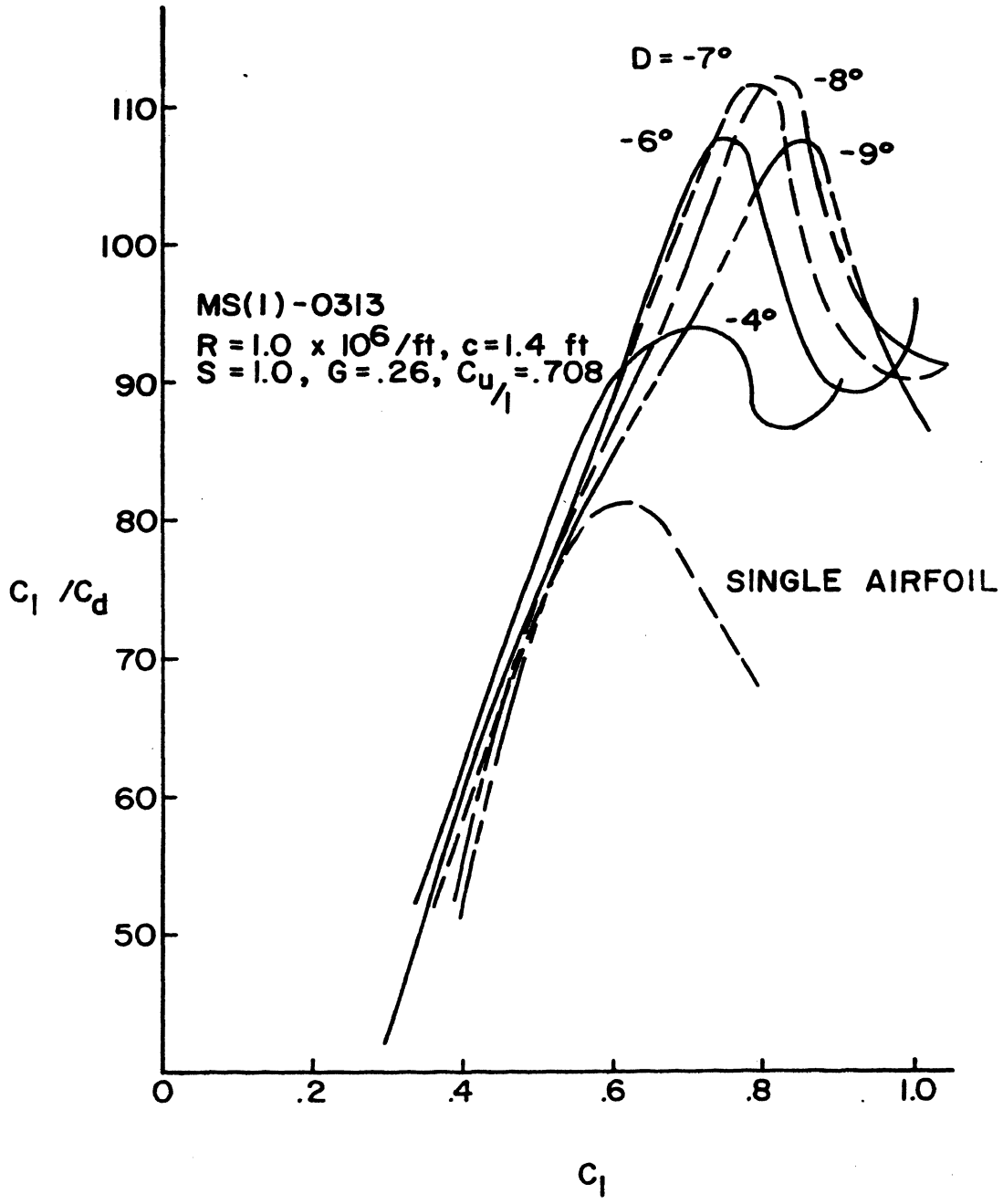

Figure 6. MS(1)-0313 Two-Dimensional Decalage Study Results for Chord Ratio Less Than One

NL(S)-0715F airfoils. Therefore, this value was used throughout the two-dimensional and three-dimensional studies of this paper.

Figure 7 shows the results obtained for the dual MS(1)-0313 airfoil section with a chord ratio greater than unity, that is the upper airfoil chord larger than the lower airfoil chord. Here the stagger was varied to maintain the upper airfoil ahead of the lower airfoil. With increasing chord ratios the maximum value of the lift-to-drag ratio was lowered. By searching for the greatest aerodynamic coupling, the chord ratio of 1.25 and 1.125 stagger was optimized through stagger and decalage variations which obtained only marginal improvements over the single MS(1)-0313 airfoil.

Summarized in Figure 8 are the optimum viscous drag results for the dual NL(S)-0715F airfoil. Compared to the previous results for the 0.708 chord ratio dual MS(1)-0313 airfoil, this dual airfoil system presents no major advantage over its single airfoil counterpart. The only noticable changes occurred at lift coefficients greater than 0.9, which are certainly above the typical cruise regime between 0.45 and 0.65. Variations in chord ratios, stagger, and decalage provided essentially no improvements over the single airfoil below lift coefficients of 0.9. However, above this value increasing the chord ratios improved the advantage of the dual airfoil.

By searching for a dual airfoil configuration which would surpass the single NL(S)-0715F airfoil resulted in the following combinations: 1) NL(S)-0715F, top airfoil, and MS(1)-0313, bottom airfoil (WNM), 2) MS(1)-0313, top airfoil, and NL(S)-0715F, bottom airfoil (WMN). The WNM configuration is summarized in Figure 9. Variations in chord ratios, stagger, and decalage had little effect upon improving the WNM

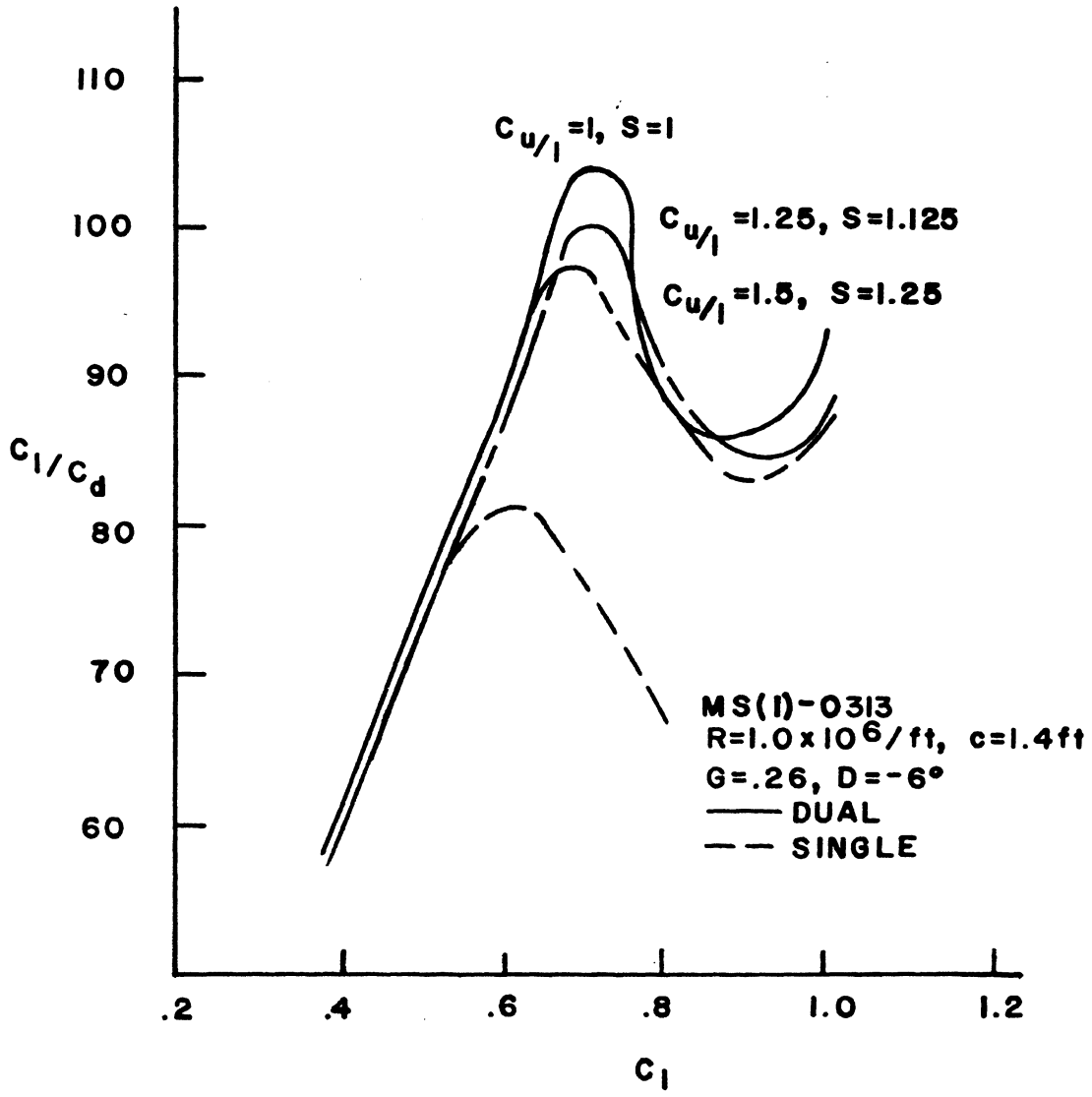

Figure 7. MS(1)-0313 Two-Dimensional Chord Ratio Greater Than One Study Results

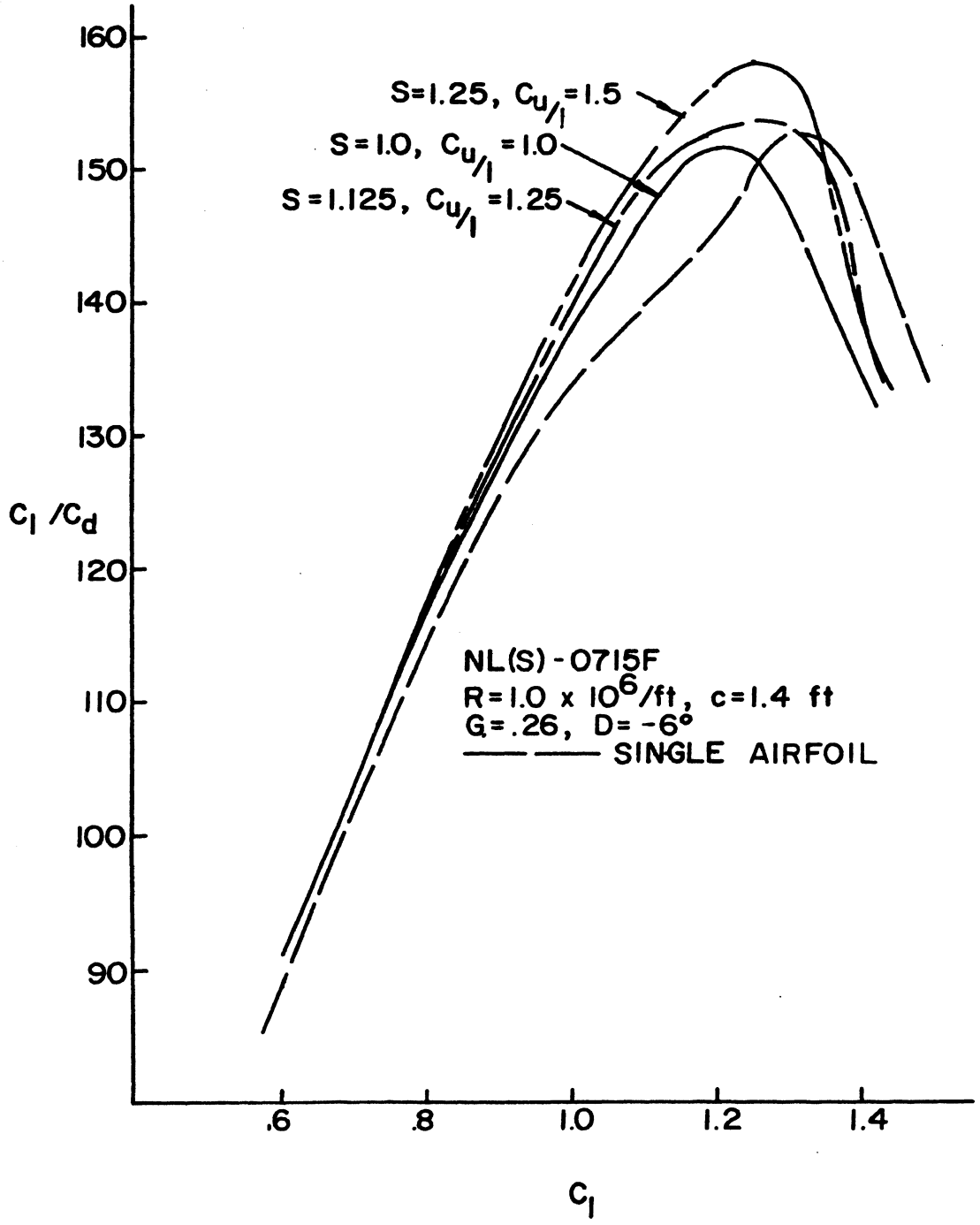

Figure 8. NL(S)-0715F Two-Dimensional Chord Ratio Greater Than One Study Results

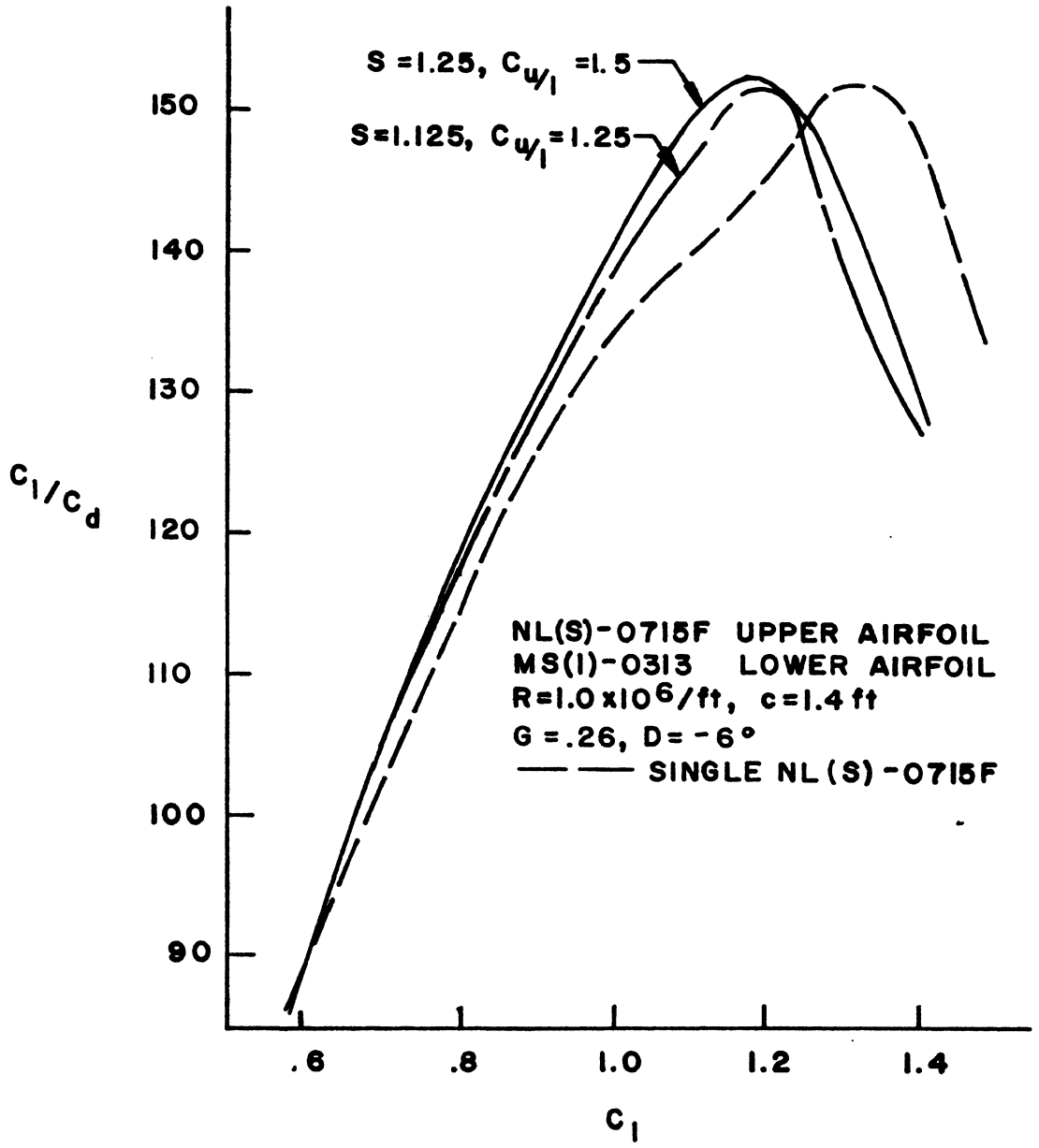

Figure 9. NL(S)-0715F and MS(1)-0313 Two-Dimensional Chord Ratio Greater Than One Study Results

system over the single NL(S)-0715F airfoil below a lift coefficient of 0.8. In addition, several of the dual airfoil systems were substantially inferior to the single NL(S)-0715F airfoil. The WMN configurations also produced poor results compared to the single NL(S)-0715F airfoil. These configurations had very little improvement over the single NL(S)-0715F airfoil throughout the stagger, decalage, and chord ratio variations.

To summarize the study of the MS(1)-0313 and NL(S)-0715F airfoils, the WNM and WMN combinations gained very little drag reduction over the single NL(S)-0715F airfoil. The dual MS(1)-0313 at S=1, G=0.26, D=-6°, and $C_{u/l}$ =0.708 obtained the highest lift-to-drag ratio in comparison with its single airfoil counterpart. This behavior for the MS(1)-0313 dual airfoils can best be explained by the transition plot, Figure 10. The transition points for both the single airfoil and dual airfoils occurred approximatley at 60% chord for low lift coefficient values and at 10% chord for high lift coefficient values. The single airfoil transitional shift happened between lift coefficient values of 0.6 to 0.8. In contrast the dual airfoils of 0.708 chord ratio transitional shift occurred at lift coefficients of 0.9 to 1.15. The importance of this behavior was that the dual airfoil maintained a longer period of laminar flow between lift coefficients of 0.6 to 1.15 and a corresponding viscous drag reduction.

In Rhodes' work (11), it was shown that the peak aerodynamic coupling occurred simultaneously with the optimum two-dimensional lift-to-drag ratio. So, for the MS(1)-0313 0.708 chord ratio case discussed above the effects of such coupling are shown in Figure 11,

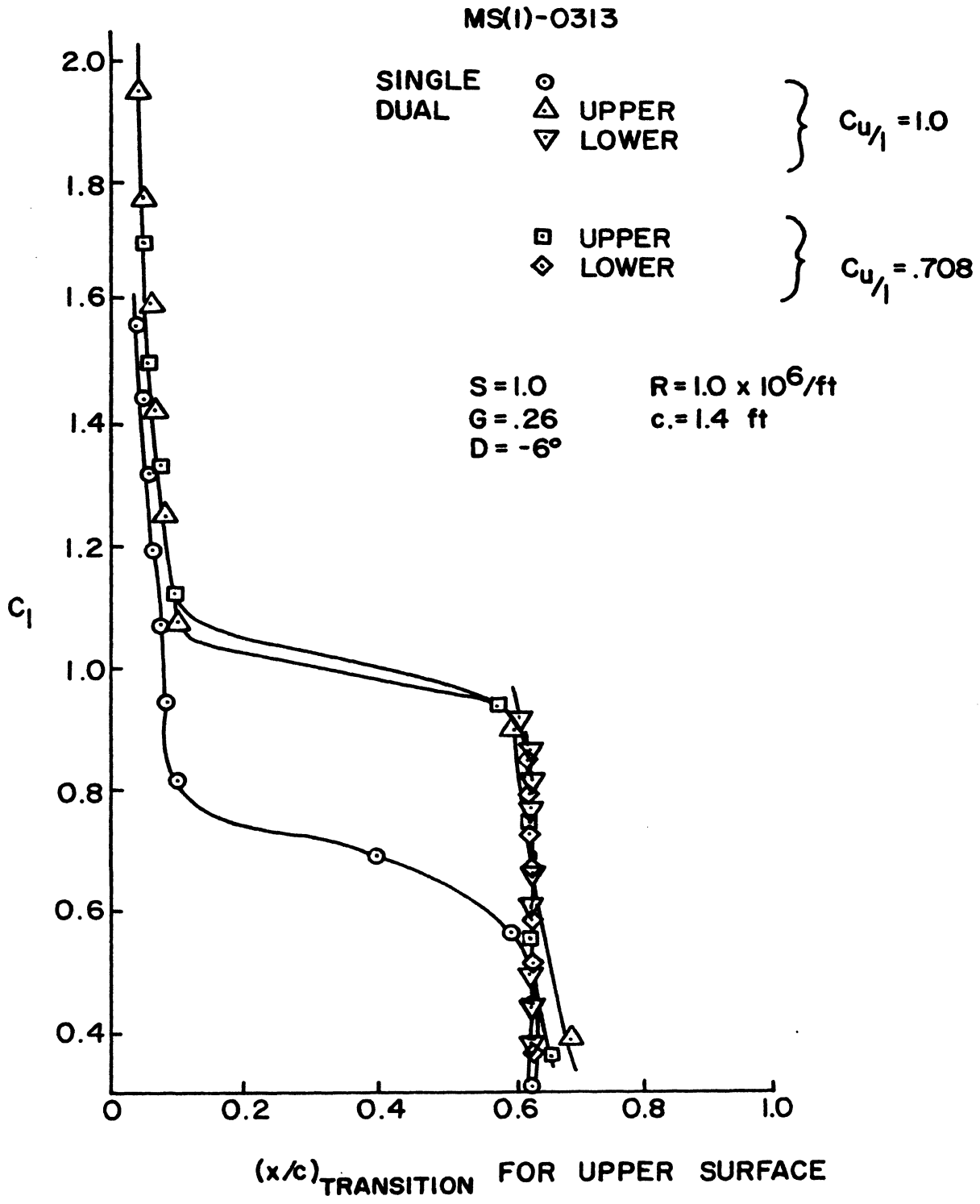

Figure 10. MS(1)-0313 Transition Points

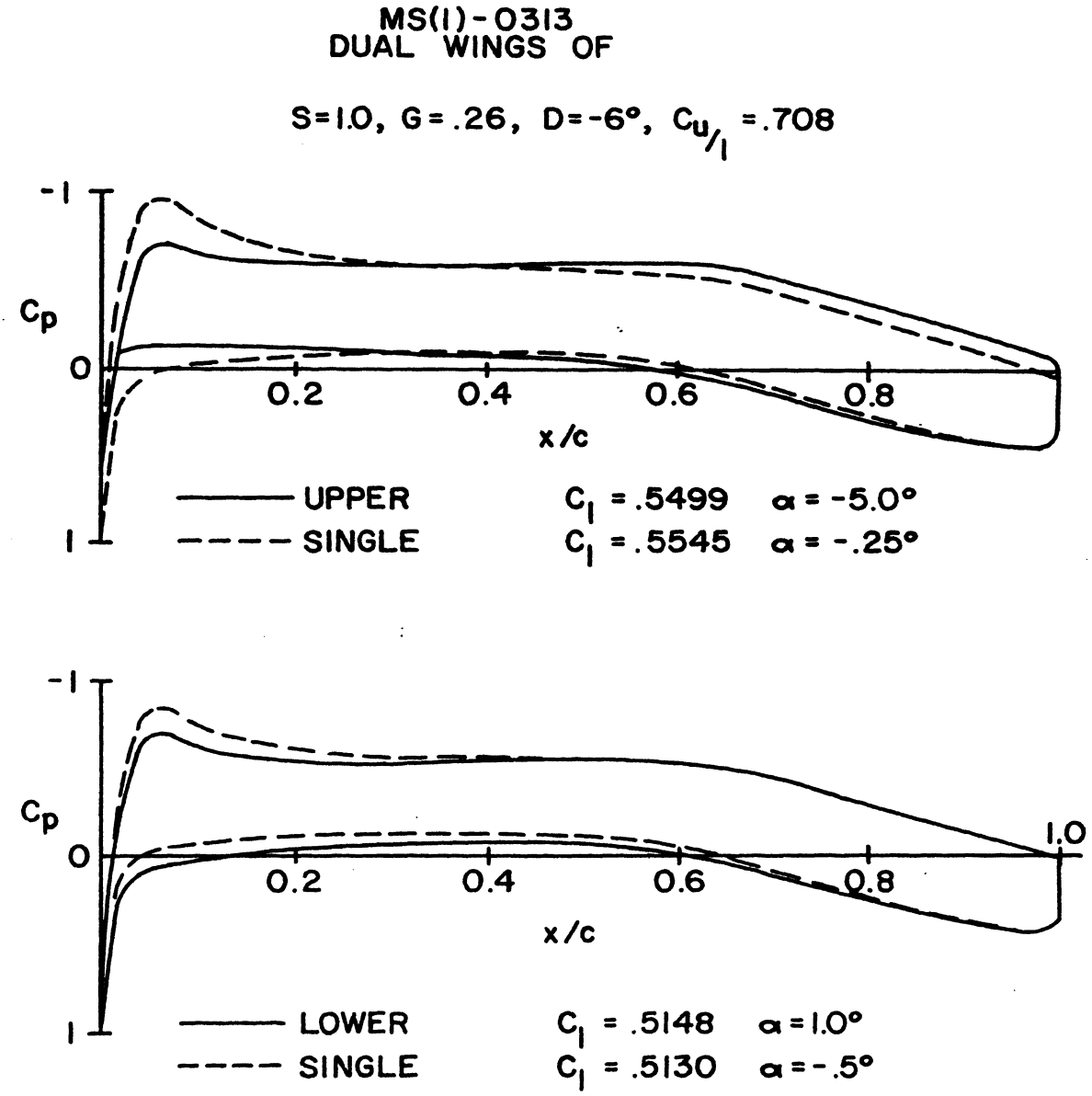

Figure 11. Single and Dual Wing Pressure Distribution

through a comparison of surface pressure distributions. The lower airfoil at a geometric angle of attack of one degree obtained a lift coefficient of 0.5148, comparable with that of a single airfoil at an angle of attack α=-0.5°. The upper airfoil produced a 0.5499 lift coefficient at a geometric angle of attack of α=-5° which is close to the single airfoil at an angle of attack of α=-0.25°. Hence, the upper and lower airfoils received a +5.25 degree and -1.5 degree induced angle of attack, respectively. In addition, the adverse pressure gradient and the leading edge pressure peak were reduced for the dual airfoils, both of which suppress boundary layer separation.

A 20% chord flapped version of the MS(1)-0313 airfoil was also investigated, as summarized in Figures 12 through 14. The drag was reduced considerably at lower lift coefficients for the δ_F=-5° flap deflection, illustrated in Figure 12. This negative flap deflection has the advantage of reducing the nose down pitching moment coefficient by 60%, yielding a lower required trim moment, hence lower trim drag. With combinations of the flapped and unflapped MS(1)-0313 airfoil, Figure 13 shows the dual airfoil study of equal chords, S=1, G=0.26, and D=-6°. With only the lower airfoil flapped, the dual airfoil drag was reduced for all lift coefficients compared to the single unflapped airfoil. When only the upper airfoil was flapped, the dual airfoil configuration was better than the single airfoil between lift coefficients of 0.45 to 0.8; elsewhere, the dual airfoils were inferior. With both airfoils flapped higher drag occurred than for the single airfoil at most lift coefficients.

From Figure 13 it was seen that both cases of the dual airfoil

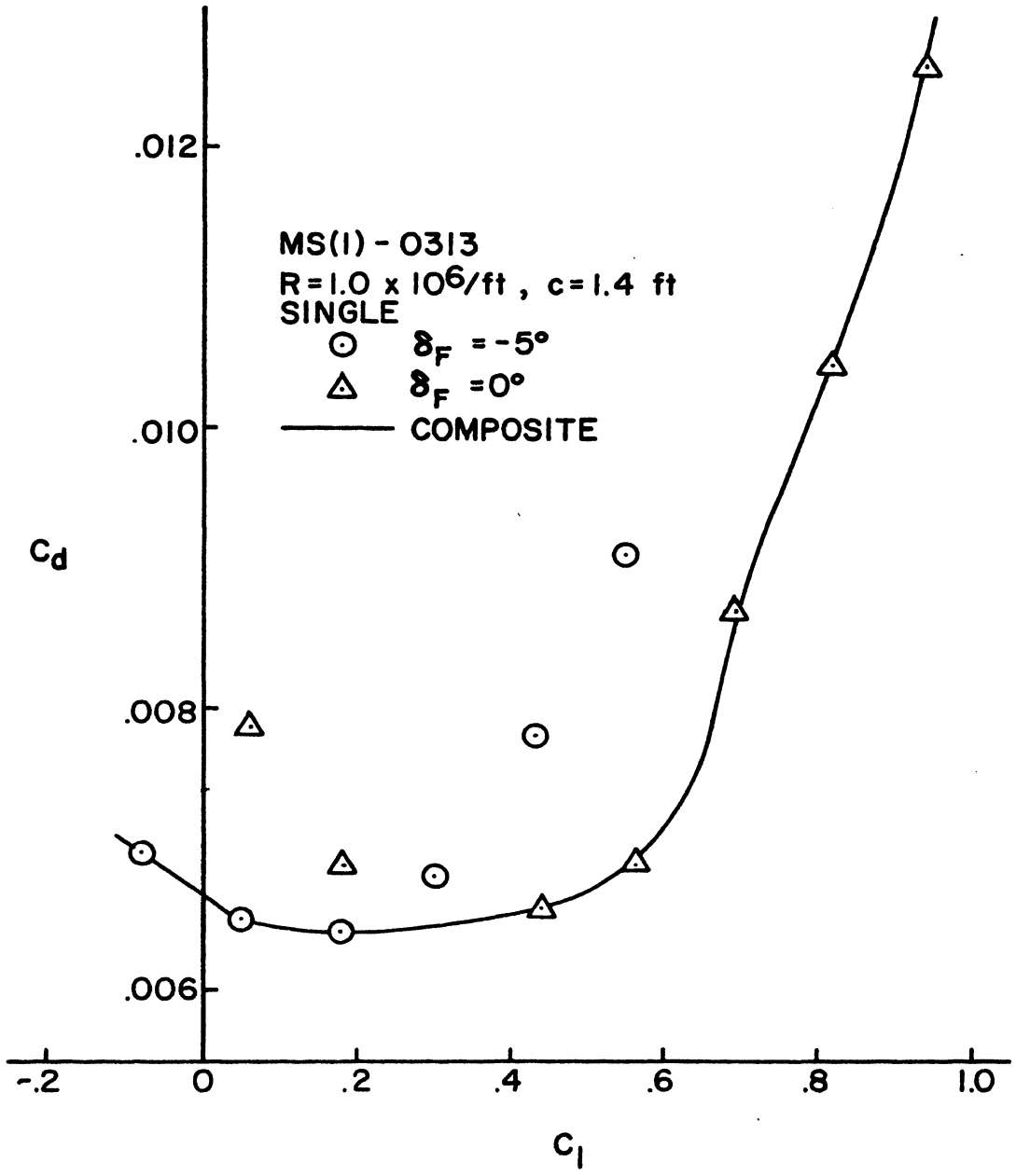

Figure 12. Single Flapped MS(1)-0313 Two-Dimensional Results

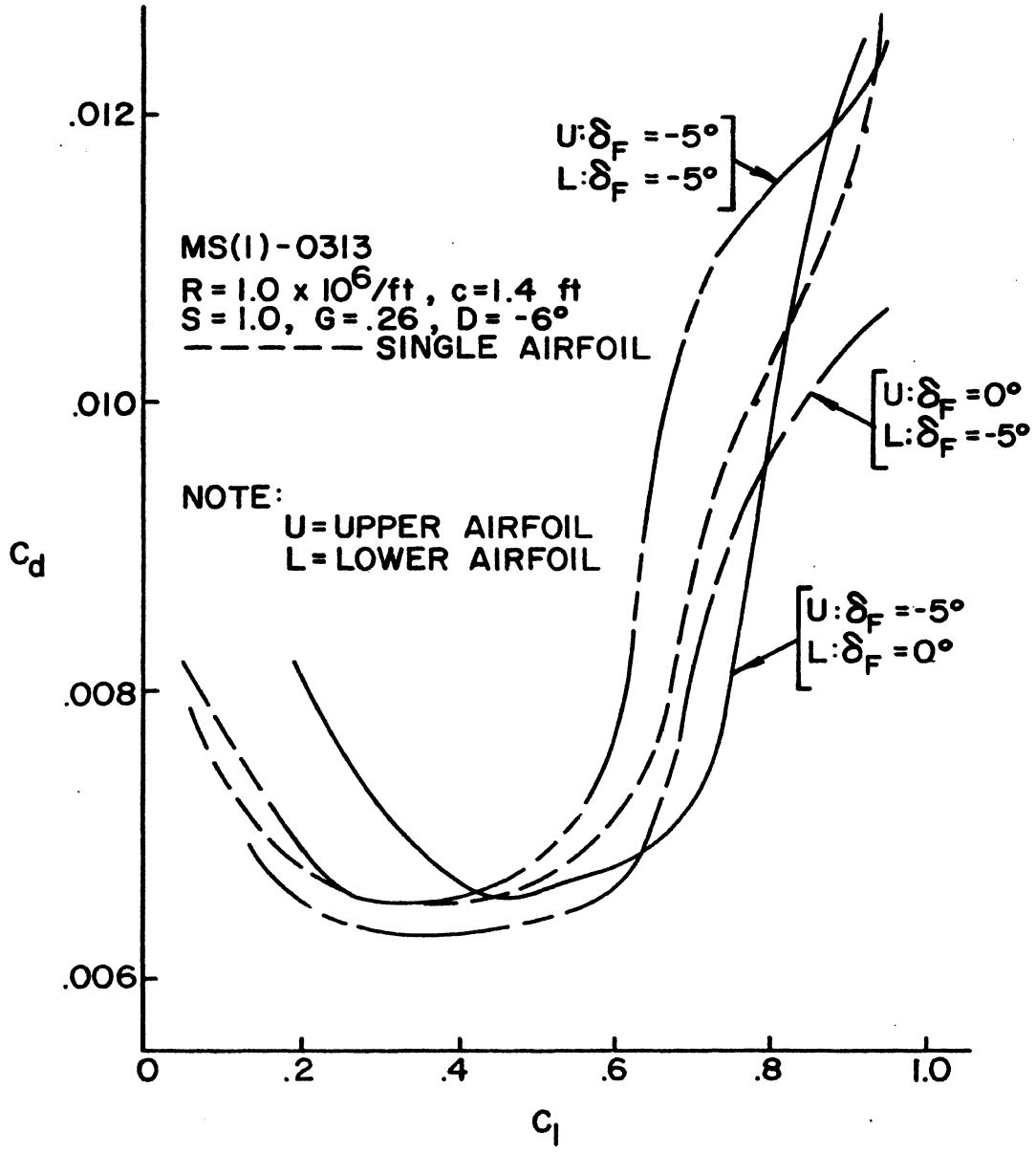

Figure 13. Dual Flapped MS(1)-0313 Two-Dimensional Study Results

with only one of the airfoils flapped produced lower drag as compared to the single airfoil for lift coefficients greater than 0.5. Since stagger had only minor effects upon the lift-to-drag ratio compared to decalage variations, the two dual airfoil configurations were optimized from chord ratio and decalage studies. Figure 14 presents the relative location of the best sectional lift-to-drag ratio results for the dual MS(1)-0313 airfoil cases. At a fixed S=1 and G=0.26 the unflapped 0.708 chord ratio case peaked above the flapped dual airfoil systems. The lower flapped dual airfoil of equal chords and D=-8° marginally out performed the upper flapped dual airfoil of 0.708 chord ratio and D=-6°. However, both flapped cases possessed higher lift-to-drag ratios than the unflapped 0.708 chord ratio case below lift coefficients of 0.6.

Both the RONCZ 1073 and 1085 were designed to have many of the characteristics of the MS(1)-0313 but optimized for a R_c=1.0x10^6. However, these dual airfoils had only marginal advantages over their single airfoil counterparts. The RONCZ 1073 and 1085 were studied at chord ratios 1.0 and 0.708 which were previously shown advantageous for the MS(1)-0313 dual airfoil. Each of the dual airfoils obtained very little drag reduction over their single airfoil below a lift coefficient of 0.9, illustrated by Figure 15. Since there were no substantial improvements over their single airfoil counterparts, no farther studies were performed using these airfoils. However, the dual airfoil results did shift the lift-to-drag ratio curves to the left, thus giving higher lift-to-drag ratios at lower lift coefficients.

The induced drag was calculated using a three-dimensional vortex

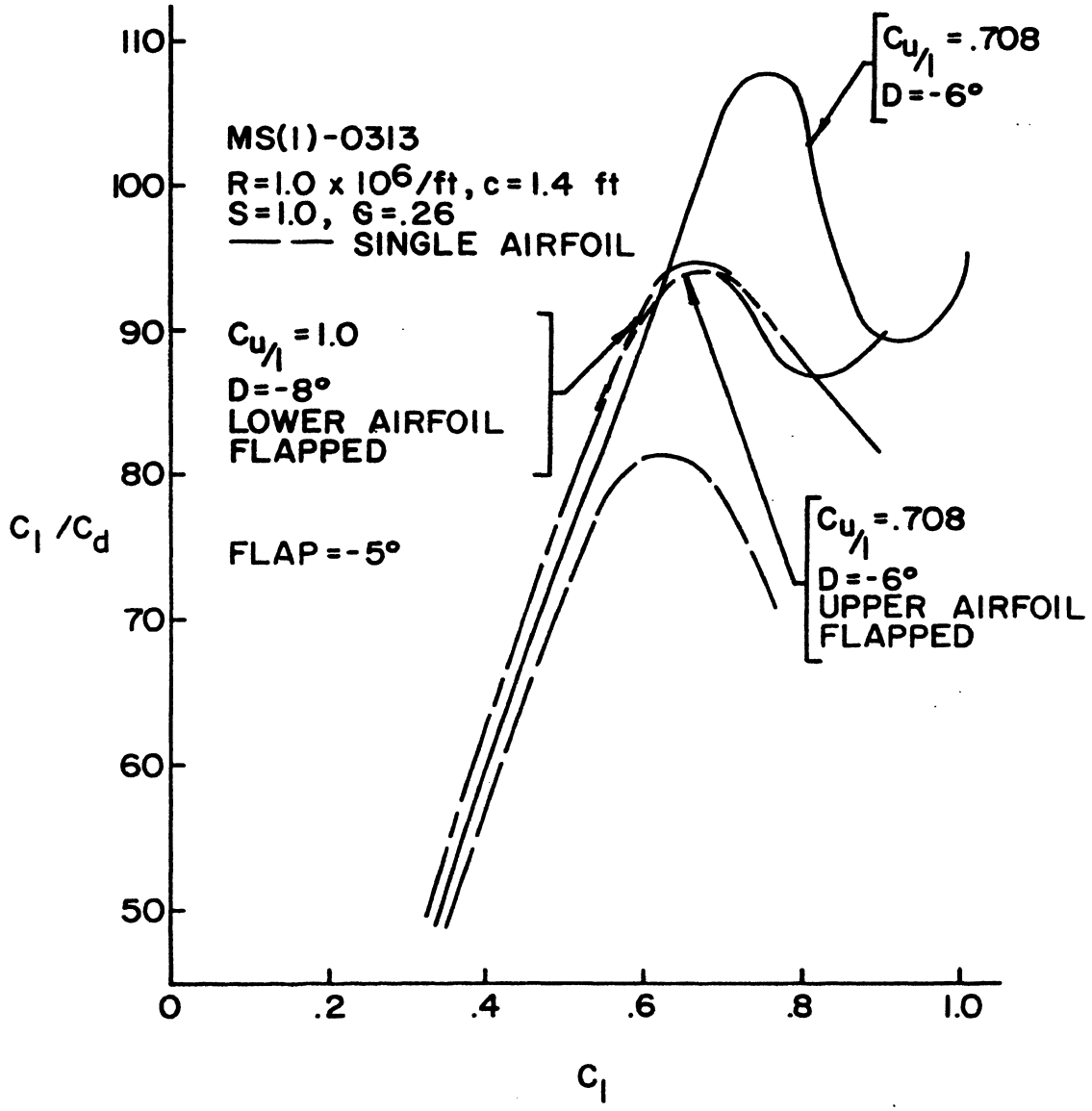

Figure 14. Dual MS(1)-0313 Two-Dimensional Summary Results

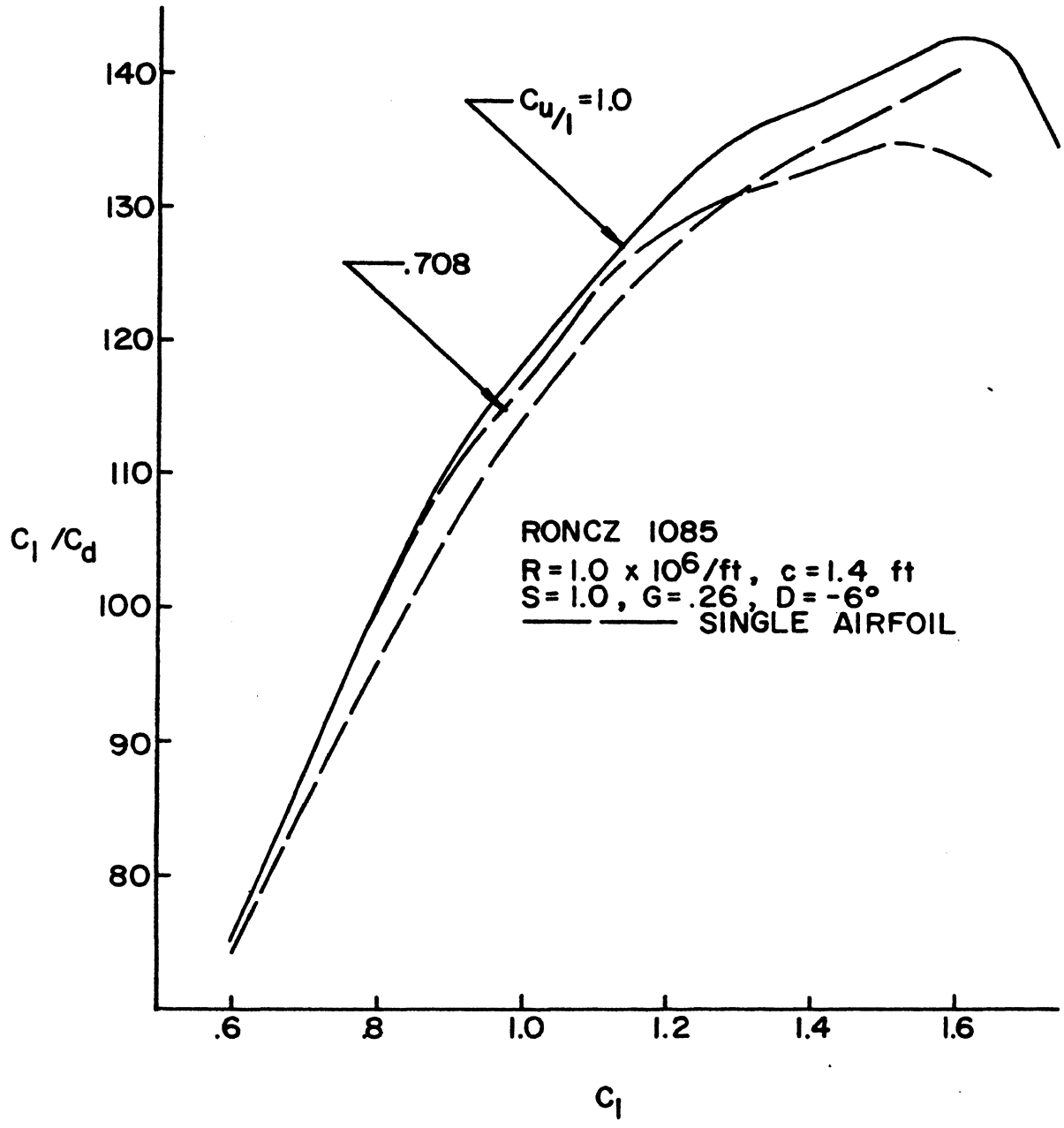

Figure 15. RONCZ 1085 Two-Dimensional Chord Ratio Study Results

lattice program. In Figure 16, the optimum case from Rhodes' study (11) was in two dimensions S=1, G=0.26, and D=-6°, and in three dimensions an aspect ratio of 16, and a taper ratio of 0.6. With the planform constant, decalage and chord ratios were varied separately. This had negligible effect upon the induced drag. Also, Rhodes (11) concluded that the two-dimensional drag difference was 70-90% greater than the induced drag difference for the cases tested. Therefore, the optimum configuration from the chord ratio studies was based upon the least amount of two-dimensional drag.

From the results of the configuration study, Figure 14 summarizes the dual airfoil systems whiched possessed the largest lift-to-drag advantage over the single airfoil below lift coefficients of 0.8. Two of the cases were chosen for more detailed three-dimensional analysis: 1) dual MS(1)-0313 airfoils of $C_{u/l}$=0.708, and D=-6°, and 2) dual MS(1)-0313 airfoils, with the lower airfoil flapped, $C_{u/l}$=1.0, and D=-8°, both of which had S=1 and G=0.26. Case 1 was selected since it peaked the highest relative to the single airfoil and to the other cases. However, case 2 obtained the highest lift-to-drag ratios for lift coefficients below 0.6. The optimum dual wing system was based upon which of the above two cases possessed the lowest total drag when placed on an equivalent six-place aircraft.

The optimum case from the total drag comparisons for the six-place aircraft was also used to design a twelve-place version. These two aircraft possessed similar characteristics to the dual wing of equal chords and single wing aircraft from Rhodes (11). Each six-place and twelve-place version of the aircraft, for reference points, used the same fuselage, aft tail, and powerplant. With these

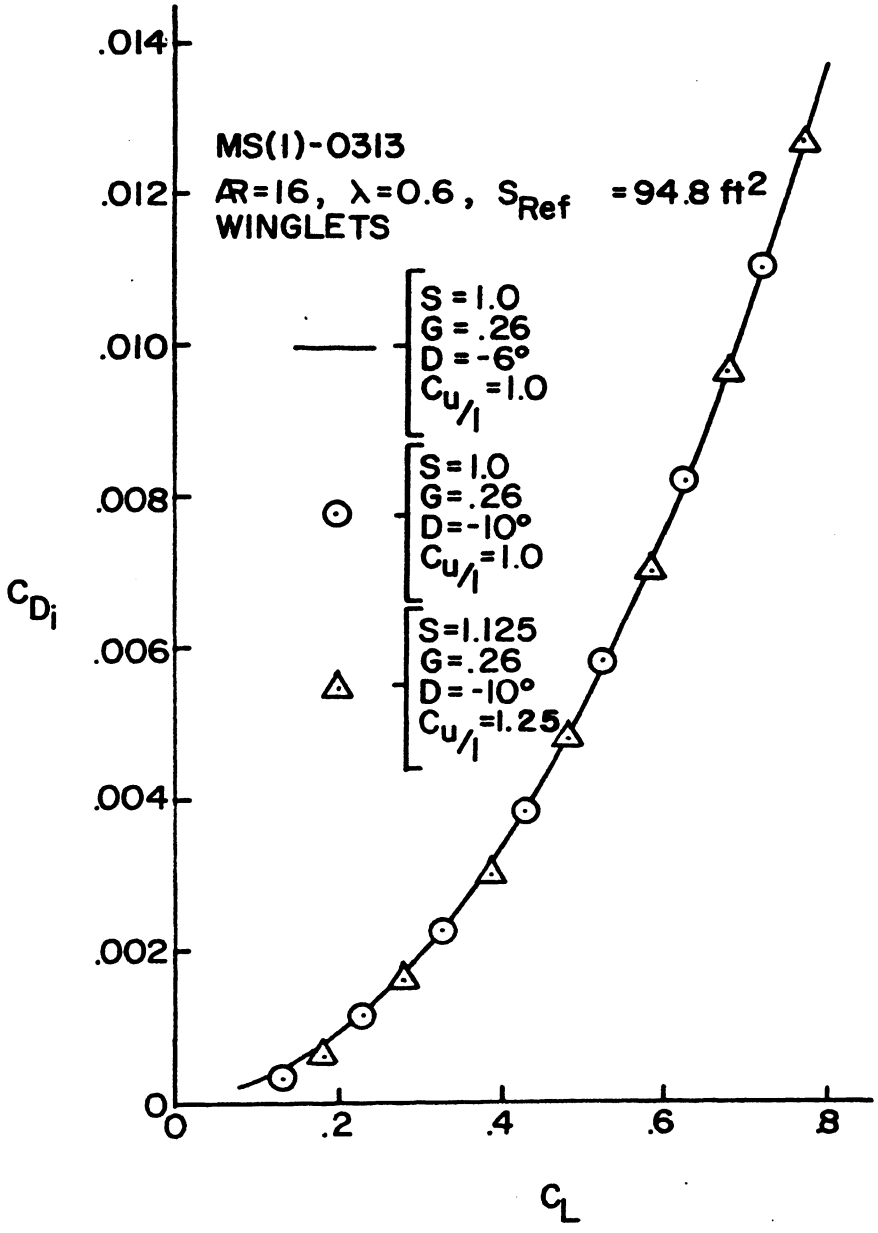

Figure 16. Chord Ratio Effects upon the Three-Dimensional Aerodynamics for the MS(1)-0313

reference points, the merits of the present dual wing design were compared to the designs of Rhodes (11).

III. DESIGN OF THE DUAL WING AIRCRAFT

The two unequal chord ratio dual wing aircraft designed in this study used the same fuselage and empennage areas of the previous study (11). By varying only the chord ratios, the benefits or penalties of unequal and equal chord ratio dual wing aircraft can be assessed. In addition, two other requirements were kept constant. First, the specifications were the same: a six-place and twelve-place version was designed for a 350 mi/hr cruise speed at altitudes of 30-40,000 ft and a range of 1500 mi or more. Second, procedures for total drag estimations, aircraft optimization, and induced drag reduction via winglets were parallel with those of the previous study (11).

The six-place turboprop version was designed for use as a personal or small business airplane with a 1200 lb payload. The turbofan twelve-place aircraft, carrying twice the payload of the six-place, was to compete in the business aircraft market. A wing aspect ratio of 16 was used maintaining structural integrity by connecting the wings at three locations: root, first bending mode antinode, and tip. In addition, all lifting surfaces were made of composite materials.

The optimum taper ratio from previous dual wing studies (11) was used as a starting point for unequal chord dual wings. Figure 17 summarizes a similar study for unequal chords. Taper ratios λ=0.6 and λ=0.4 possessed lower induced drag than λ=0.8. A taper ratio of λ =0.6 was chosen over λ=0.4 in this study because the MS(1)-0313 airfoil was designed for high Reynolds numbers, and the λ=0.4 would result in small chords, hence low Reynolds numbers.

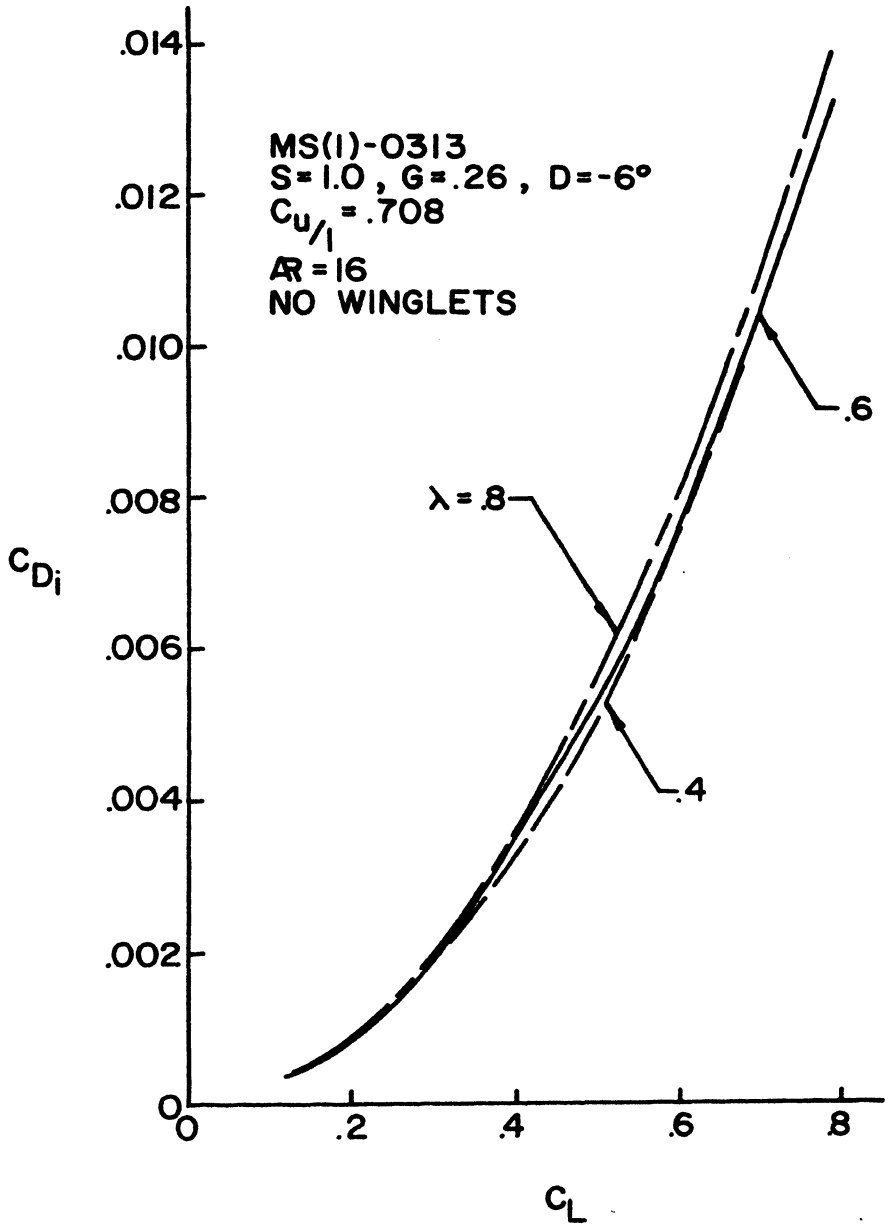

Figure 17. Taper Ratio Effects on the Induced Drag

The weights of the components for the six-place and twelve-place aircraft were consistent with those of Rhodes' design (11) except for the wing and engine weights. The engine weights were scaled according to the following method. The turboprop engine weight was based upon the ratio of required power to rated production power, and the turbofan engine weights were scaled by the ratio of required thrust to reference engine thrust. The dual wing was connected at three locations to prevent spanwise variations in decalage for the whole wing assembly. With a factor of safety of 1.5, and ultimate load factor of 5.7 calculated from a 3.8g load, dual wing weights were minimized by Somnay (22). Modifications to these wing weights were made to account for composite material.

Figure 18 summarizes the output from the wing area optimization program. For reference, the six-place aircraft with the planform shown was used to compare the equal and unequal chord dual wings. Aspect ratios 12 and 16 for the single and dual wing, respectively, were tested at 40,000 ft since Rhodes (11) proved these configurations resulted in the least drag. Also, winglets were added to all the aircraft for an induced drag reduction. The dual MS(1)-0313 wing with the lower wing flapped possessed higher cruise drag than the 1.0 and 0.708 chord ratio cases. However, the 0.708 chord ratio obtained the least amount of cruise drag over the other aircraft around a reference area of 89 sq ft. An MS(1)-0313 monoplane of aspect ratio 12 and taper ratio of 0.8 was used as the reference aircraft in assessing the benefits or penalties of the dual wing design. The dual wing of 0.708 chord ratio was placed on a twelve-place aircraft instead of the flapped MS(1)-0313 dual wing since the former possessed lower total

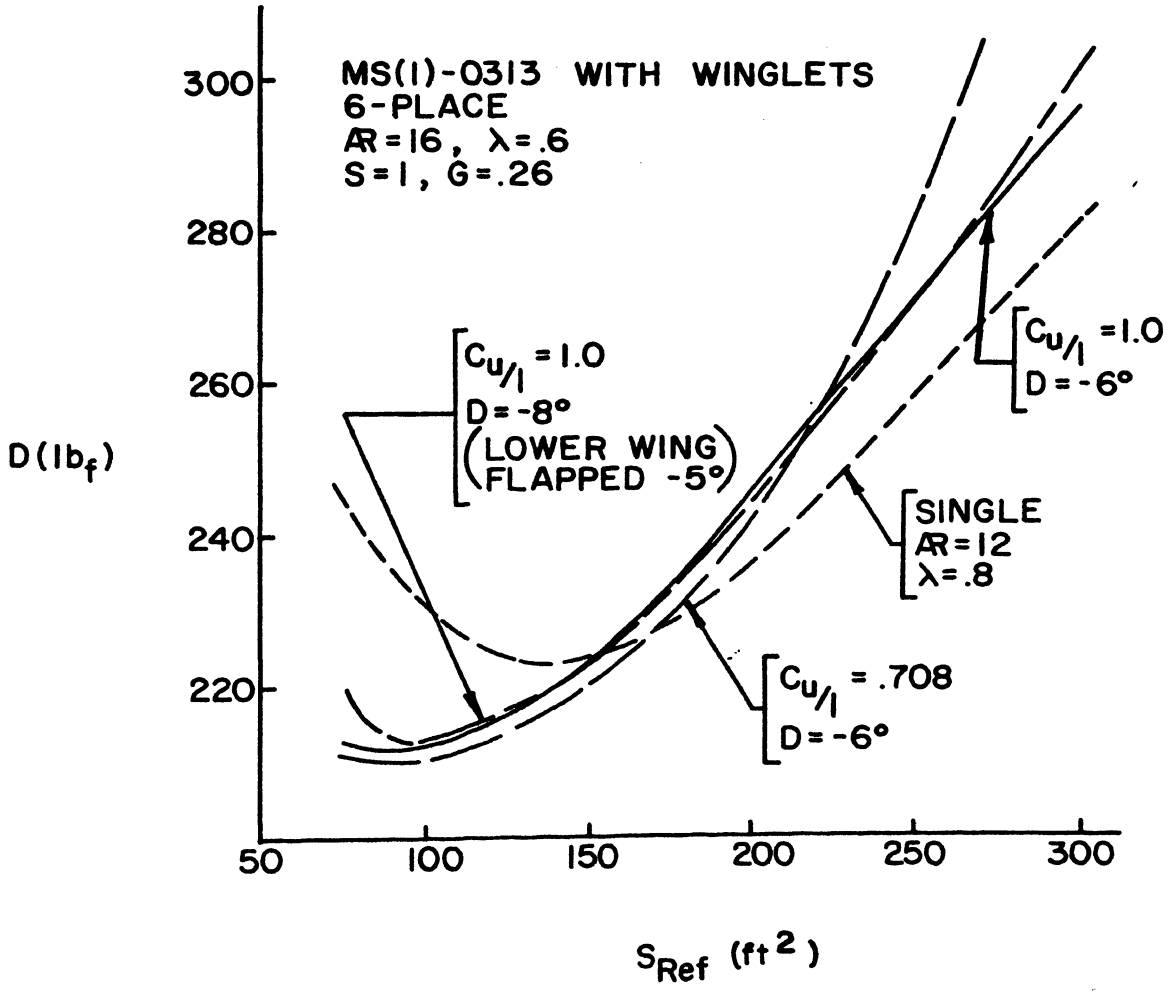

Figure 18. Six-Place Optimization Curves

drag. A variable aspect ratio study, Figure 19, illustrates that the largest aspect ratio possible, 16, for the unequal chord dual wing produces the least induced drag coefficient, hence a lower total aircraft drag coefficient. Similar total drag results were found for the twelve-place aircraft.

With knowledge of the optimum wing area, the areas of the horizontal and vertical tail for the aircraft were checked to insure that longitudinal, lateral, and directional static stability was maintained. By placing the aircraft center of gravity at its most unfavorable position, the assumed horizontal and vertical tail areas were checked for static stability. The static stability analysis was performed using the techniques of Roskam (24,25) and Torenbeek (26). The results from this analysis were found to be comparable with those of typical light aircraft. No dynamic stability analysis was conducted in this study.

By using this horizontal tail area, the trim performance of each aircraft was estimated. The required tail lift coefficient at cruise was calculated to obtain a zero moment coefficient about the aircraft center of gravity. For this tail lift coefficient, the tail drag coefficient was obtained from the momentum integral boundary layer and vortex lattice programs. This additional drag increment was calculated and added to the untrimmed results. A new engine weight was found using this total trimmed drag. With this weight change a revised optimum wing area was computed via the program mentioned previously to obtain the final trimmed aircraft results.

The results from this parametric study are summarized in Table I. Designs of Rhodes (11), the baseline case and dual wing of 1.0 chord

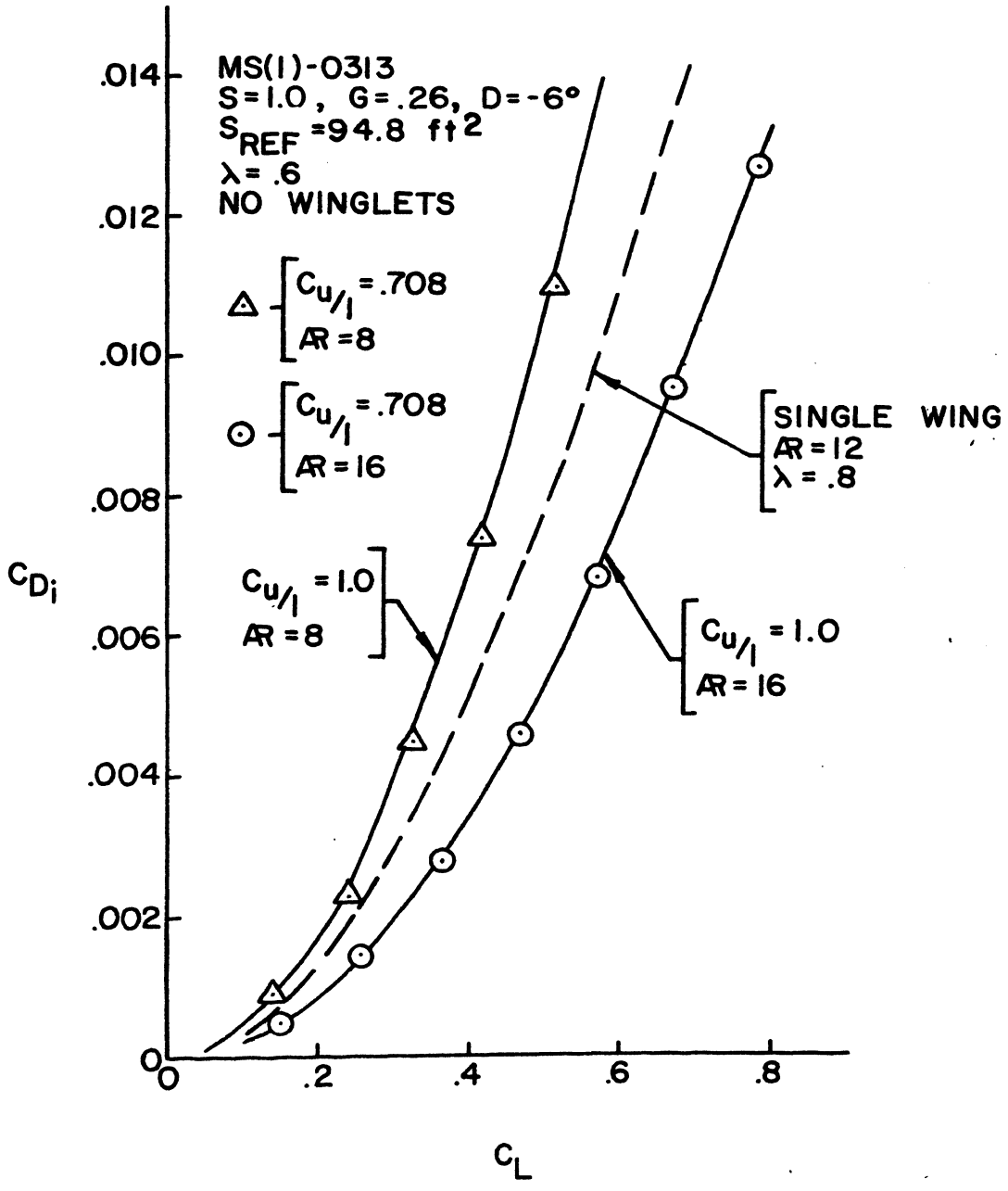

Figure 19. Three-Dimensional Aerodynamics of Chord Ratio Variations

TABLE I. AIRCRAFT DESIGN PERFORMANCE

	W_{cr} lb	W_{ENG} lb	W_{WING} lb	$C_{L_{cr}}$	D_{cr} lb	P_{REQ} hp	$\frac{\Delta P_{REQ}}{P_{REQ}}$ %	$\left(\frac{L}{D}\right)_{cr}$	S_{REF} ft^2	$\left(\frac{W}{S}\right)_{WING}$	R mi	$\frac{\Delta R}{R}$ %
TRIMMED 6-PLACE WITH WINGLETS												
MS(1)-0313												
SINGLE WING BASELINE	4625	806	429	0.41	236	220		19.71	146.8	31.5	1675	
DUAL WING OF CHORD RATIO												
1.0	4476	748	338	0.66	216	202	-8.2	20.50	87.2	51.3	1800	7.5
0.708	4481	746	345	0.62	215	201	-8.6	20.60	93.0	48.2	1807	7.9
TRIMMED 12-PLACE WITH WINGLETS												
SINGLE WING BASELINE	8484	867	887	0.46	431	402		19.74	239.4	35.4	1737	
DUAL WING OF CHORD RATIO												
1.0	8320	827	763	0.57	385	360	-10.4	21.51	188.4	44.2	1936	11.5
0.708	8321	825	766	0.56	383	357	-11.2	21.71	192.4	43.2	1950	12.3

ratio, are shown for comparison. Both six-place and twelve-place designs of the aircraft are trimmed at cruise conditions. The table presents estimates of: total weight, wing and engine weights, lift coefficient, drag, required power, lift-to-drag ratio, wing area, wing loading, and range. Also, the required power and range are compared to the baseline design by percentage differences.

Performance of the six-place 0.708 chord ratio dual wing aircraft was marginally superior to the 1.0 chord ratio dual wing aircraft. When referenced to the baseline design, the percentage differences in range for the 0.708 chord ratio aircraft was greater than the 1.0 chord ratio aircraft. This improvement resulted from lower drag hence lower required power for the 0.708 chord ratio dual wing design. Similar trends occurred for the twelve-place 0.708 chord ratio dual wing aircraft. Between the two dual wing aircraft, the 0.708 chord ratio possessed the lower wing loading which would improve its stall performance at lower flight speeds, an area not covered in this study.

Figure 20 shows the exterior view of the finished six-place dual wing aircraft of 0.708 chord ratio.

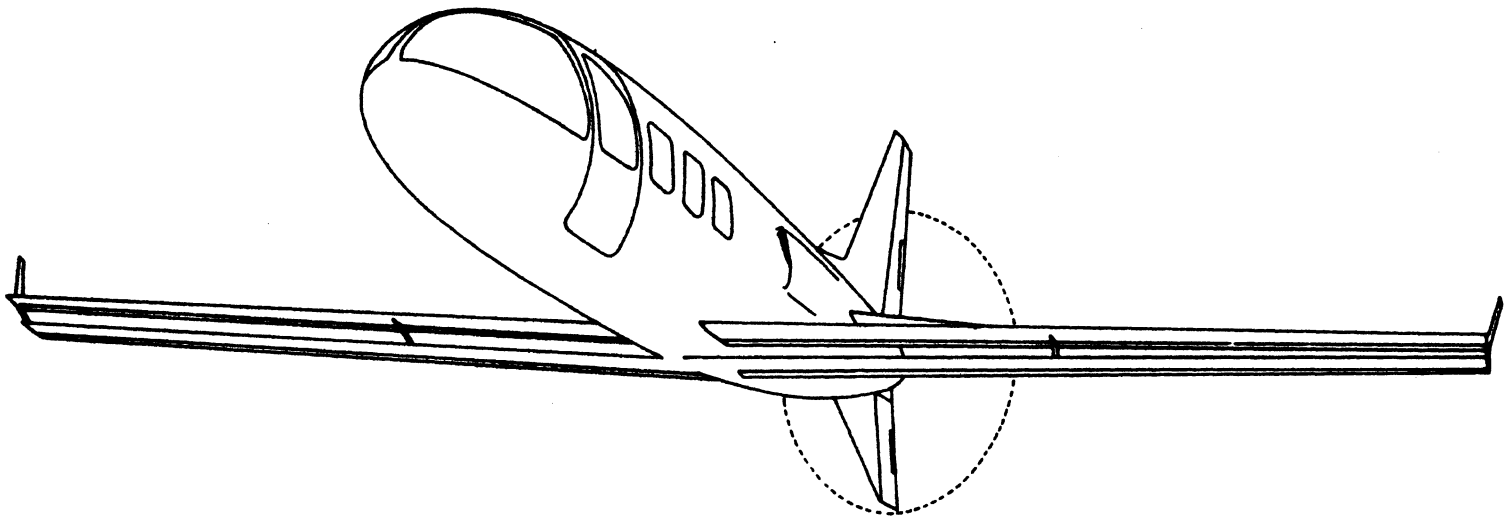

Figure 20. Dual Wing Design Exterior Views

IV. DESIGN COMPARISON AND RECOMMENDATIONS

From Table I, the dual wing aircraft possessed lower drag compared to the single wing aircraft. The six-place version obtained approximately a 9% drag reduction and the twelve-place reached a 11% drag reduction over their single wing counterparts. At a lower cruise drag, the dual wing aircraft required less power than the baseline designs, hence lower engine weight. From this weight reduction, the range for both dual wing aircraft reached a value of 12% above the baseline designs. Throughout this comparison the dual wing of unequal chords, 0.708 chord ratio, was marginally superior to the equal chord design.

The superior behavior of the dual wing of 0.708 over the dual wing of 1.0 chord ratio originated from the sectional characteristics. From Figure 19, the three-dimensional comparisons of the dual wing aircraft both possessed similar induced drag results at high and low aspect ratios. However, from Figure 4 the 0.708 chord ratio obtained higher sectional lift-to-drag ratios over the 1.0 chord ratio. This behavior was also reflected in Figure 10 where the 0.708 chord ratio maintains a longer period of laminar flow than the 1.0 chord ratio, therefore superior sectional characteristics.

A few potential problems exist in using the dual wing design. Higher stall speeds resulting from small wing areas, summarized in Table I, present possible low speed problems especially for take off and landing performance. Inadequate wing volume forced some fuel to be carried by the fuselage. Aeroelastic instability, an area not covered in this study, could be possible with these large wing aspect

ratios.

Attempts were made to best utilize the dual wing of 0.708 chord ratio. From Table I, the highest cruise lift coefficient was 0.62 for the 0.708 dual wing case. However, Figure 4 illustrates the optimum sectional lift-to-drag ratio occurs around a lift coefficient of 0.75. To increase the cruise lift coefficient, deviations were made from the design criteria mentioned previously.

Figure 21 summarizes the off design conditions and how they affect the cruise lift coefficient. Variations in altitude and velocity are illustrated, while the baseline six-place design is shown for comparison. The most apparent results are the higher cruise lift coefficients for the dual wing compared to the single wing aircraft. In addition, the dual wing aircraft obtained a 15% increase in the fuel efficiency versus the single wing aircraft at lower velocities. For the dual wing aircraft at an altitude of 30,000 ft, reducing the velocity from 350 to 250 mph increased the mpg by 45%, when trimmed at the highest cruise lift coefficient, 0.68.

Applications for an unequal chord ratio dual wing aircraft appear to be at slower speeds. At a speed of 150 mph, the dual wing aircraft obtained the largest mpg improvement, 15%, over the single wing aircraft. This improvement resulted from the dual wing aircraft optimizing at higher Reynolds numbers. Use on the agriculture aircraft appears attractive, because high cruise lift coefficients are required throughout most of the aircraft's flight.

Since the 0.708 chord ratio case produced only small gains over the 1.0 chord ratio case, it would be advantageous to use the latter, for high Reynolds number airfoils. The 0.708 chord ratio case

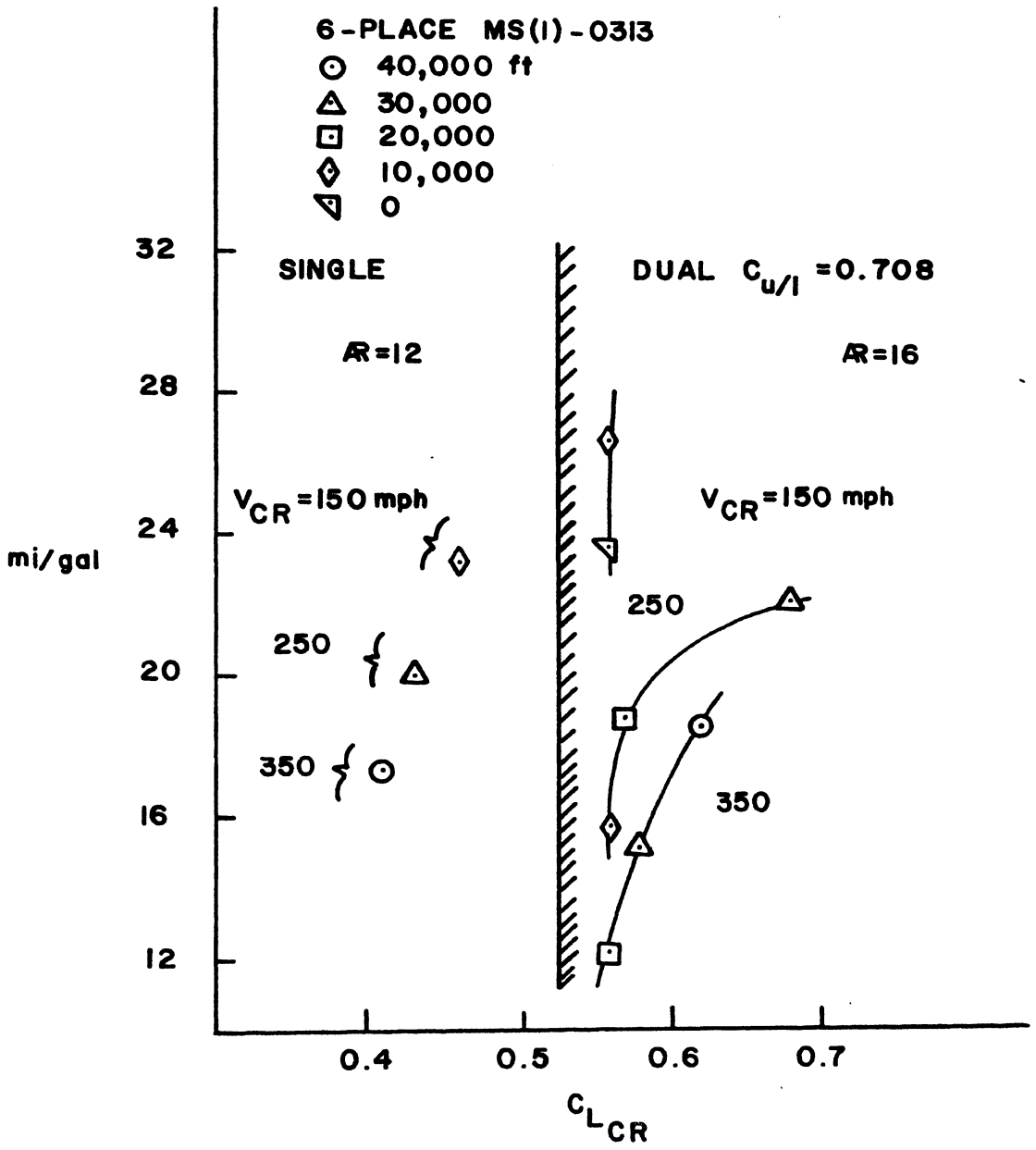

Figure 21. Fuel Efficiency of the Dual Wing Aircraft

resulted in smaller chords than the 1.0 chord ratio case, therefore leading to lower Reynolds numbers.

For future dual wing studies, airfoils could be designed especially for the dual wing aircraft, instead of using airfoils previously designed for single wing aircraft. Also, airfoils designed for a Reynolds number range $1.0x10^6<R_c<2.0x10^6$ would improve the dual wing aircraft performance, especially for the 0.708 chord ratio aircraft. The dissimilar airfoil and unequal chord ratio results were in most cases substantially inferior to the single airfoil. However, Figure 9 illustrated for the WNM case possible combinations of dual wings producing higher lift-to-drag ratios than the single NL(S)-0715F airfoil at lower cruise lift coefficients. Similarly, the RONCZ 1085, Figure 15, at a chord ratio of 1.0 had higher lift-to-drag ratios at lower lift coefficients for the dual airfoil compared the single RONCZ 1085 airfoil. From these configurations it is concluded that an airfoil designed to be specifically tailored for dual wing purposes, by pressure distributions, could certainly lead to dual wing aircraft designs substantially superior to the monoplane.

ACKNOWLEDGEMENT

The results presented in this thesis were obtained from research funded by NASA Research Grant NAG1-26 administered by Langley Research Center.

REFERENCES

1. Norton, F. H., "Effect of Staggering a Biplane," NACA TN-710, 1918.

2. Knight, and Noyes, R. W., "Wind Tunnel Tests on a Series of Biplane Wing Models, Part I. Effects of Changes in Stagger and Gap," NACA TN-310, 1929.

3. Knight, and Noyes, R. W., "Wind Tunnel Tests on a Series of Biplane Wing Models, Part II. Effects of Changes in Decalage, Dihedral, Sweepback, and Overhand," NACA TN-325, 1929.

4. Knight, and Noyes, R. W., "Wind Tunnel Tests on a Series of Biplane Wing Models, Part III. Effects of Changes in Various Combinations of Stagger, Gap, and Decalage," NACA TN-330, 1929.

5. Prandtl, L. and Tietjens, O. G., Applied Hydro- and Aeromechanics, Dover Publications, Inc., New York, 1957, pp. 213-216.

6. Garrick, I. E., "Potential Flow About Arbitrary Biplane Wing Sections," NACA Report No. 546, 1935.

7. Nenadovitch, M., "Recherches sur les Cellules Biplane Rigides d'Envergure Infine," Publications Scientifiques et Techniques du Minister de L'Air, Institut Aero'-technique de Saint-Cyr, Paris, 1936.

8. Olson, E. C. and Selberg, B. P., "Experimental Determination of Improved Aerodynamic Characteristics Utilizing Biplane Wing Configurations," Journal of Aircraft, Vol. 13, April 1976, pp. 256-261.

9. Smith, A. M. O., "High-Lift Aerodynamics," AIAA Paper No. 74-939, 1974.

10. Rokhsaz, K.,and Selberg, B. P., "Analytical Investigation of the Aerodynamic Characteristics of Dual Wing Systems," UMR Thesis, Rolla, MO, 1980.

11. Rhodes, M. D., "Advantages of Dual Wing Aircraft Designs," UMR Thesis, Rolla, MO, 1982.

12. Roncz, J., personal communication, 1982.

13. Thwaites, B., "Approximate Calculation of the Laminar Boundary Layer," Aero. Quarterly I, 1949.

14. Michel, R., "Etude de la Transition sur les Profiles d'Aile; Establissement d'un Critere de Determination de Point de Transition et Calcul de la Trainee de Profile Incompressible," ONERA Rept. 1/1578A, 1951.

15. Cebeci, T. and Bradshaw, P., Momentum Transfer in Boundary Layers, Hemisphere Publishing Corp., Washington, 1977, pp. 192-194.

16. Cebeci, T. and Smith, A. M. O., "Calculation of Profile Drag of Airfoils at Low Mach Numbers," Journal of Aircraft, Vol. 5, Nov.-Dec. 1968, pp. 535-542.

17. McGhee, R. J., "Wind Tunnel Results for a 13-Percent-Thick Medium Speed Airfoil Section," (NASA TM in publication).

18. Somers, D. M., Data on general aviation natural laminar flow airfoil, to be published by NASA.

19. Holmes, B. J., and Croom, C. C., "Aerodynamic Design Data For a Cruise-Matched High Performance Single Engine Airplane," SAE Paper 810625, 1981.

20. Benstein, E. H., and Smith, R., "Advanced General Aviation Turbine Engine (GATE) Study," NASA CR-159624, 1979.

21. Nicolai, L. M., Fundamentals of Aircraft Design, METS, Inc., San Jose, CA, 1975, pp. 5.1-5.24, 20.1-20.24.

22. Somnay, Rajesh J., personal communication, 1982.

23. Roskam, J., Methods for Estimating Drag Polars of Subsonic Airplanes, published by the Author, Lawrence, KS, 1971, p 2.3.

24. Roskam, J., Methods for Estimating Stability and Control Derivatives of Conventional Subsonic Airplanes, published by the Author, Lawrence, KS, 1971, pp. 21.-12.2.

25. Roskam, J., Airplane Flight Dynamics and Automatic Flight Controls, Part I, Roskam Aviation and Engineering Corp., 1979, pp. 243-377.

26. Torenbeek, E., Synthesis of Subsonic Airplane Design, Delft University Press, 1976, pp. 27-76, 263-302, 352.

VITA

Gary Don Vincent was born on June 12, 1959. He received his primary and secondary education in Bay, Arkansas, graduating second in his high school class in May 1977. In August of that year, he entered the University of Missouri-Rolla as an Aerospace Engineering major. In May 1981, he received a degree of Bachelor of Science in Aerospace Engineering, Summa Cum Laude.

Since then he has been enrolled in the Graduate School at University of Missouri-Rolla, and has held the Chancellor's Fellowship since May 1981. He is a member of the National Aerospace Honor Society, the National Engineering Honor Society, and is a student member of AIAA.

APPENDICES

APPENDIX A

MS(1)-0313 DUAL AIRFOIL

The following material illustrates the details of the dual airfoil parametric studies. The dual MS(1)-0313 airfoil case for a chord ratio of 1.25 and S=1.125 was chosen for farther investigations, since extensive study was previously conducted on the equal chord ratio case (11).

By holding all other parameters fixed, stagger was varied to find the optimum case. Figure 1 shows the S=1.125 case slightly above the other cases. Also, the 1.125 case maintained the equivalence of the single airfoil at lower lift coefficients. However, the other values, 1.0 and 1.25, fell below their single airfoil counterpart.

Decalage variations for a constant 1.25 chord ratio, S=1.125, and G=0.26 are illustrated in Figure 2. Cases between D=-8 and D=-11 degrees obtained higher lift-to-drag ratios. However, their maxima occurred at lift coefficients greater than the D=-6 degree case. These lift coefficients were beyond the typical cruise lift coefficient range of 0.4 to 0.65. Also, these decalages fell below the D=-6 degree case at lower lift coefficients, hence below the single airfoil.

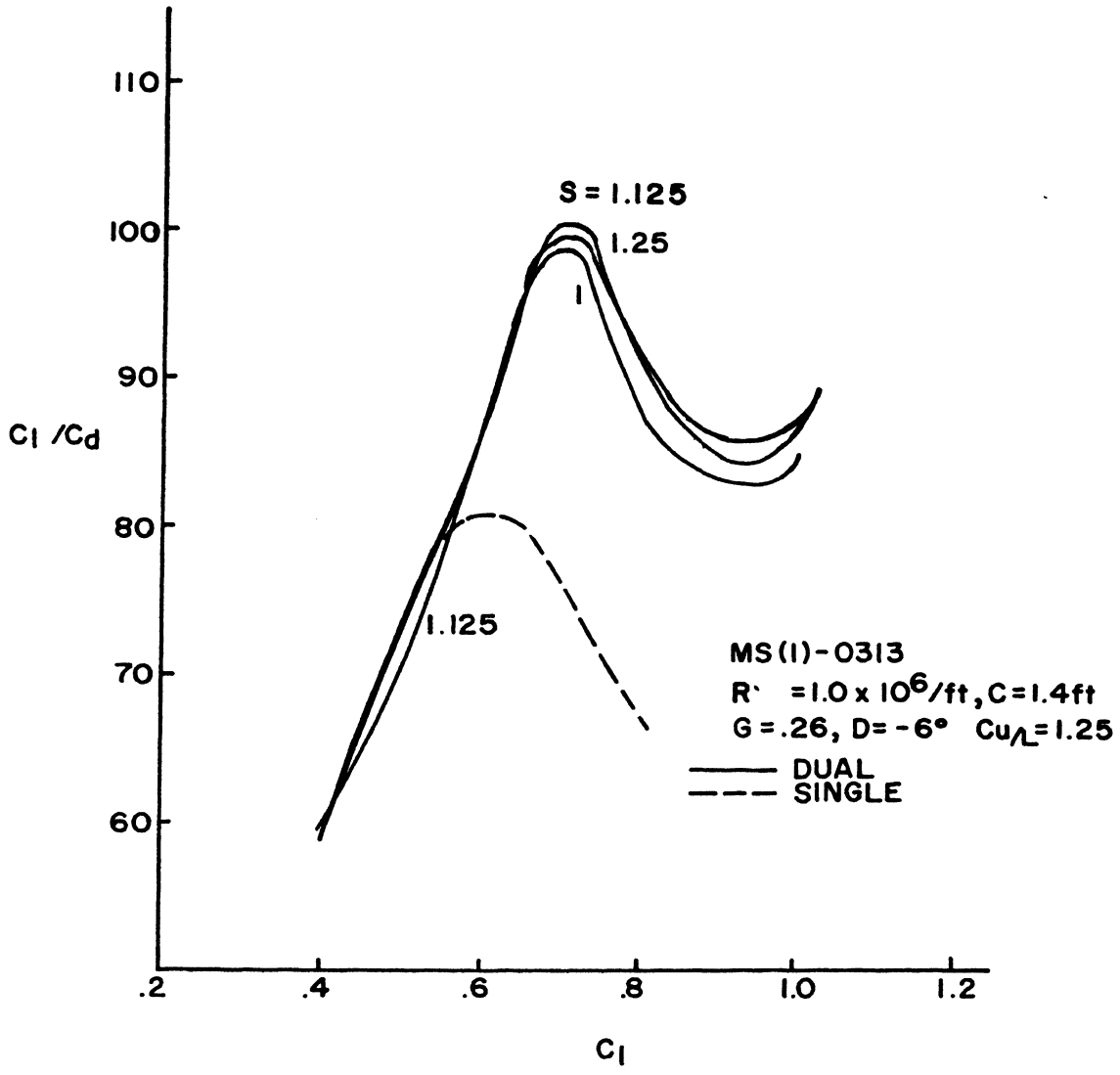

Figure 1. MS(1)-0313 Two-Dimensional Stagger Study Results for a Chord Ratio of 1.25

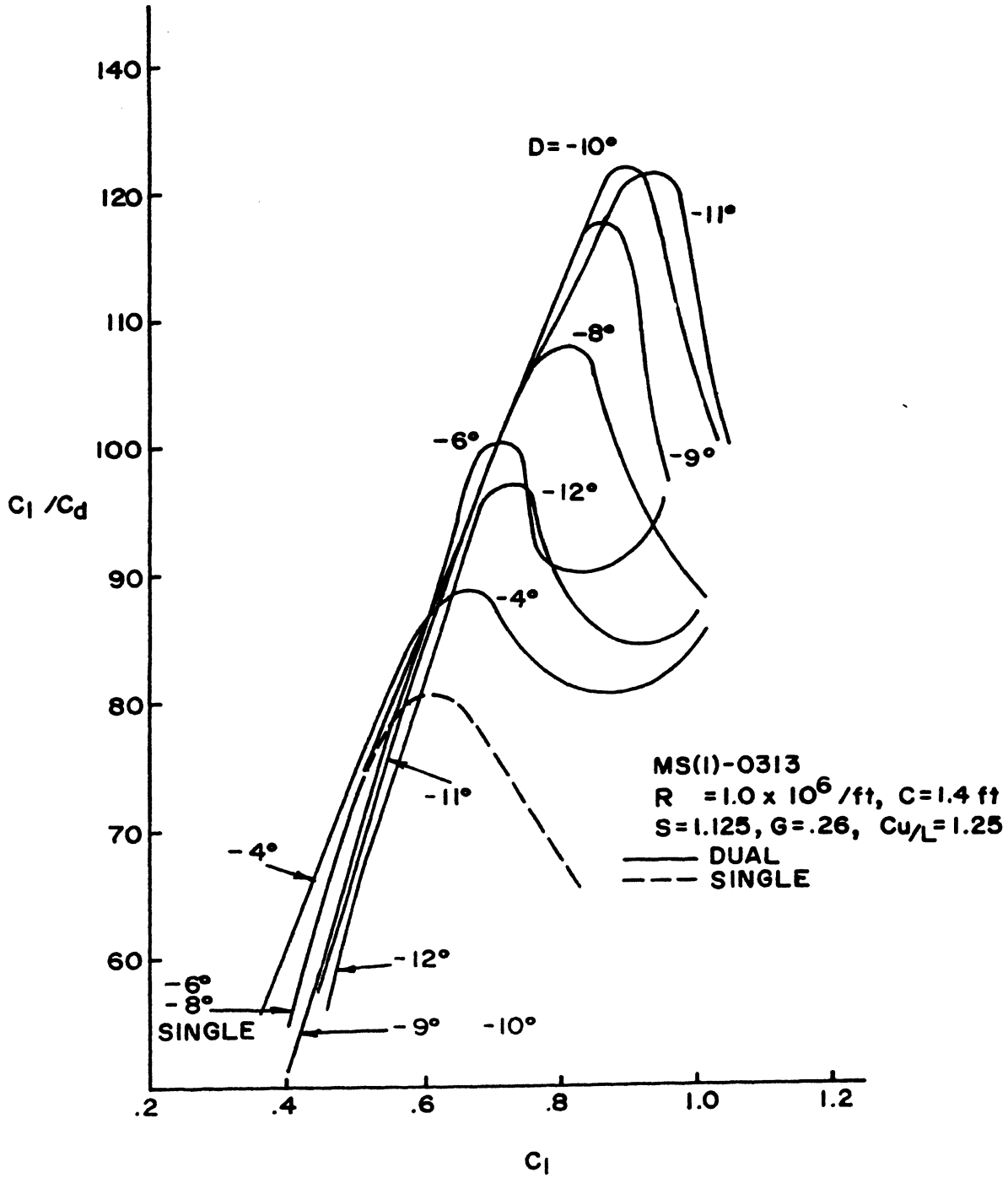

Figure 2. MS(1)-0313 Two-Dimensional Decalage Study Results for a Chord Ratio of 1.25

APPENDIX B

NL(S)-0715F DUAL AIRFOIL

Figures 1 through 3, show the viscous drag results for the two NL(S)-0715F airfoils of chord ratios less than one. Figure 1 illustrates the small effects which variable chords have upon the NL(S)-0715F airfoil. The only noticeable changes occurred at lift coefficients greater than 0.9 which are certainly above the typical cruise regime. A chord ratio of 0.6 was selected arbitrarily for the airfoils' sensitivity to variations in stagger and decalage.

Two-dimensional variable stagger and decalage studies are summarized in Figures 2 and 3, respectively. The stagger variations, Figure 2, shifted the lift-to-drag ratio curves only for lift coefficients greater than 0.9. Below this value there was little gained in the dual system over the single airfoil. Similar results were found for the decalage variations, Figure 3. For the range tested, the D=-6 degree case shifted the lift-to-drag curve farthest left for lower lift coefficients. Other decalages altered the curves for lift coefficients of 0.8 and greater.

As done for the two MS(1)-0313 airfoils, a chord ratio study greater than one was performed on two NL(S)-0715F airfoils. Figures 4 and 5 present the fine tuned stagger and decalage studies, respectively, for the two NL(S)-0715F airfoils at a 1.5 chord ratio. In Figure 4, stagger was altered around the 1.25 value. All stagger results except the 1.25 case intersected the single airfoil lift-to-drag ratio curve around the lift coefficient of 0.6. For lift coefficients greater than 0.6 there existed some improvements with the dual

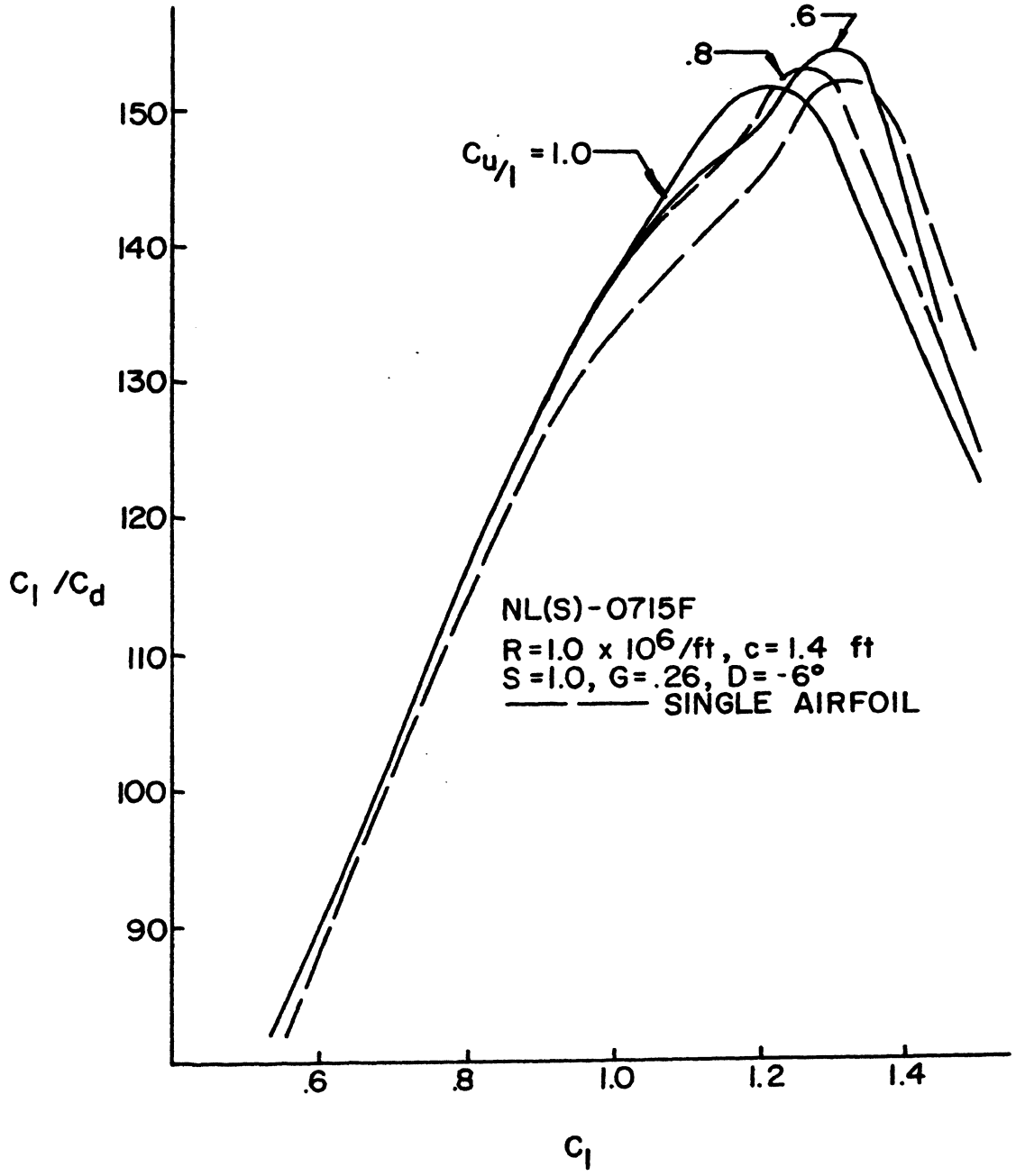

Figure 1. NL(S)-0715F Two-Dimensional Chord Ratio Less Than One Study Results

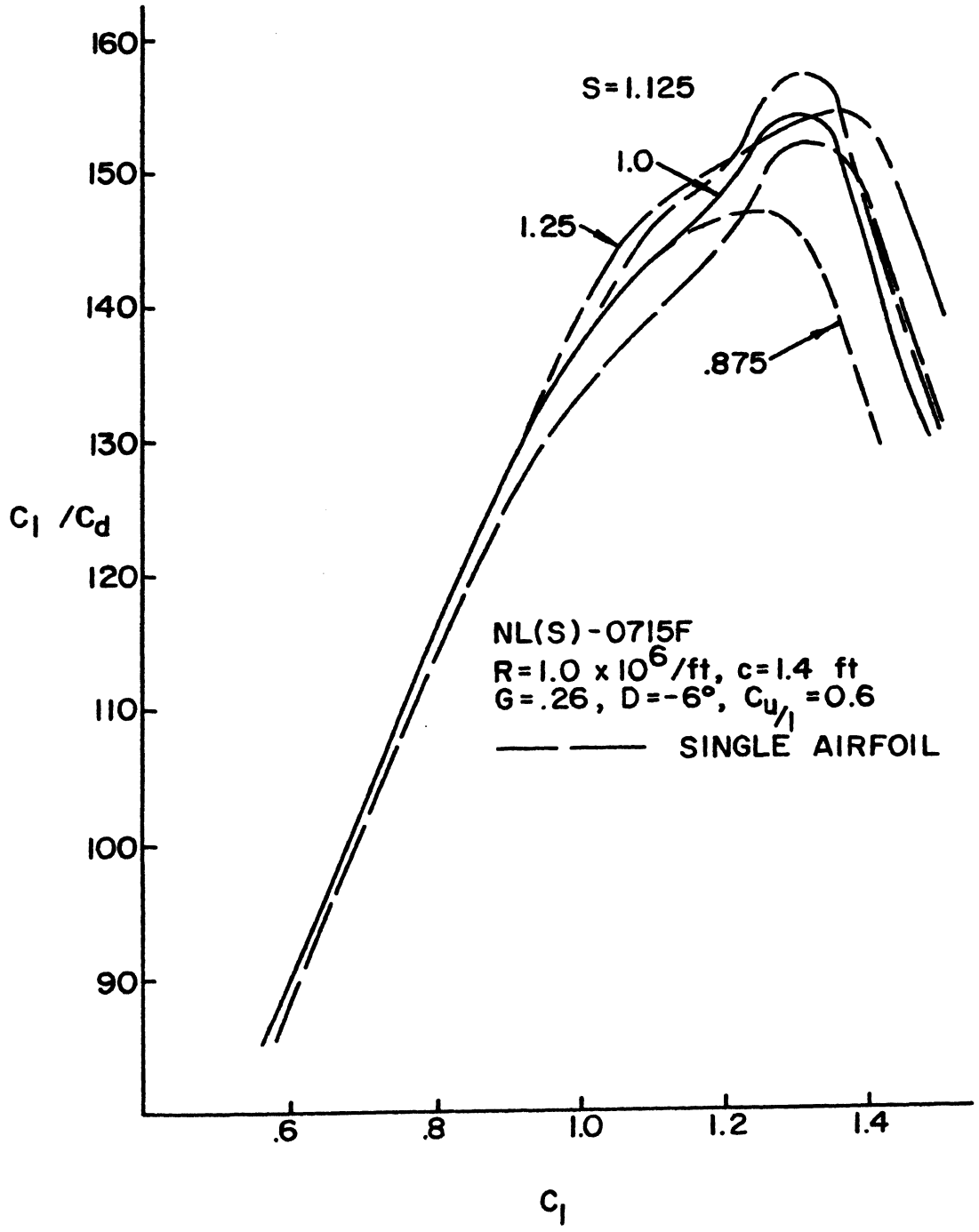

Figure 2. NL(S)-0715F Two-Dimensional Stagger Study Results for a Chord Ratio of 0.6

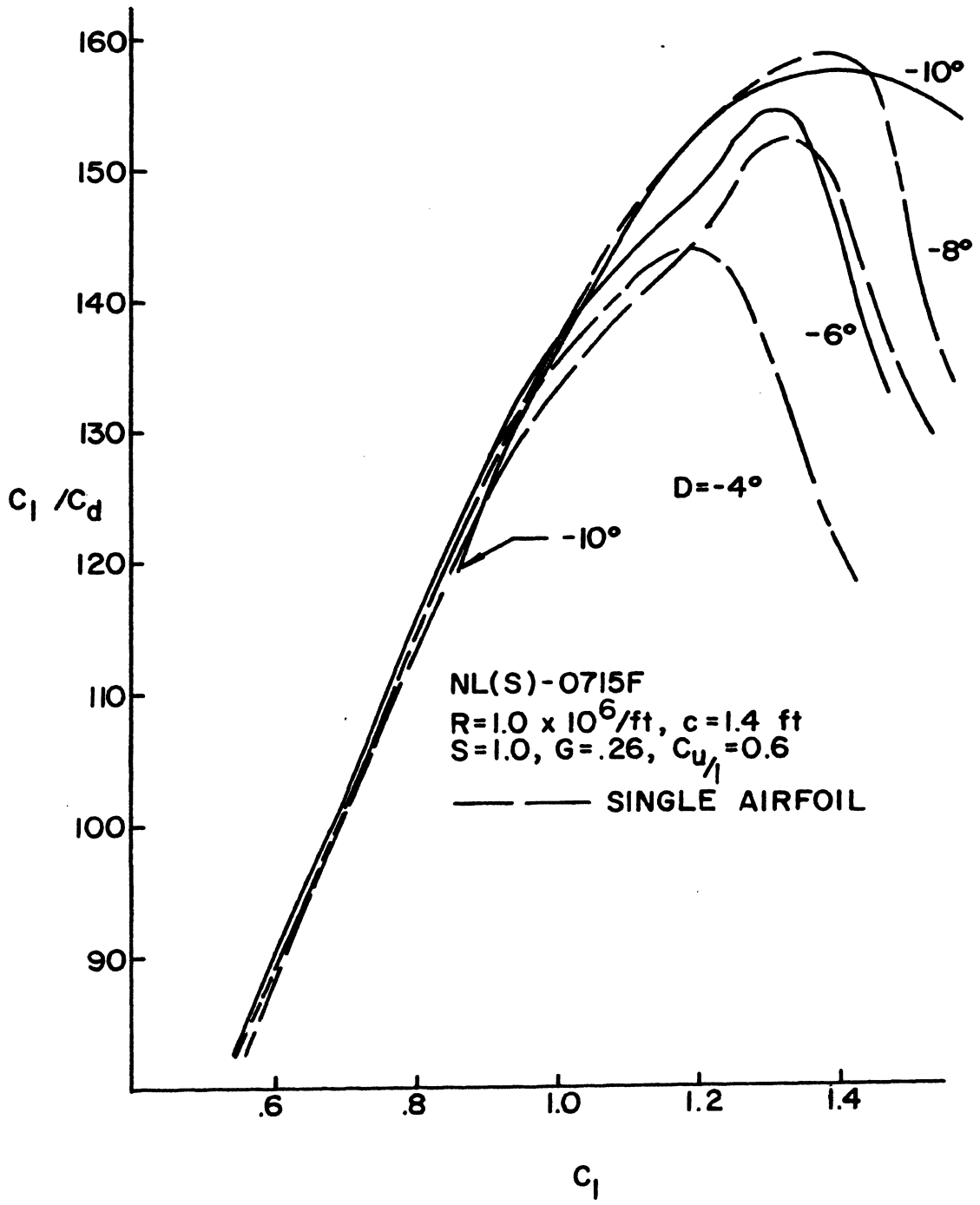

Figure 3. NL(S)-0715F Two-Dimensional Decalage Study Results for a Chord Ratio of 0.6

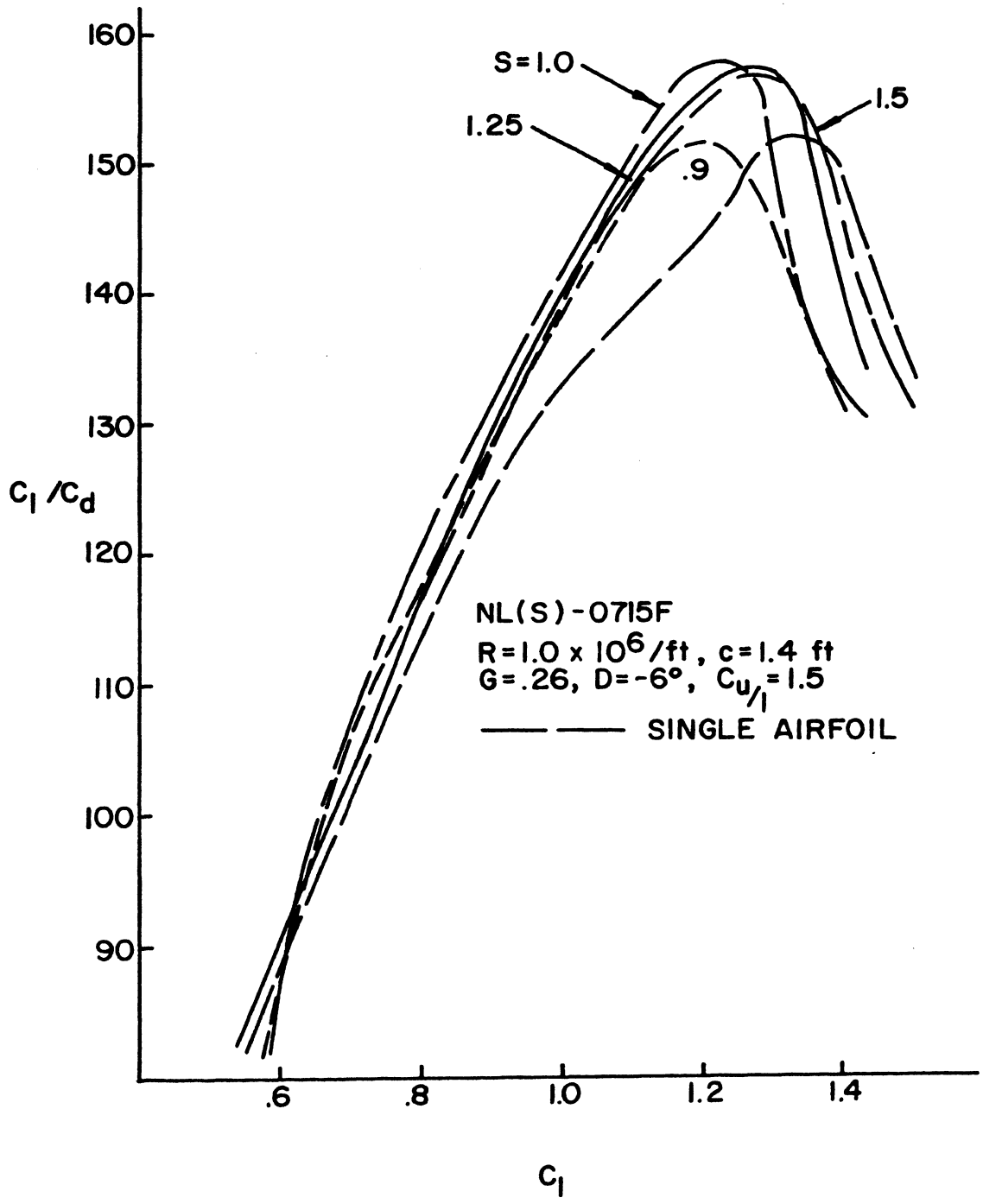

Figure 4. NL(S)-0715F Two-Dimensional Stagger Study Results for a Chord Ratio of 1.5

airfoil. As mentioned earlier, this advantage occurred beyond the typical cruise regime. However, a S=1.25 proved best relative to the other cases at lower lift coefficients. With a constant S=1.25 and 1.5 chord ratio, decalage was varied yielding the data shown by Figure 5. For the range plotted, D=-8 degrees rose above the D=-6 degree case. However, at lower lift coefficients the D=-8 degree results intersected the single airfoil results around lift coefficient of 0.7. Similarly, the D=-6 degree maintained only a small advantage over the single airfoil below lift coefficients of 0.8. Compared with Figures 1 through 3, the dual airfoil of chord ratios greater than one maintained a small advantage over the single airfoil throughout the parametric study in the typical cruise region.

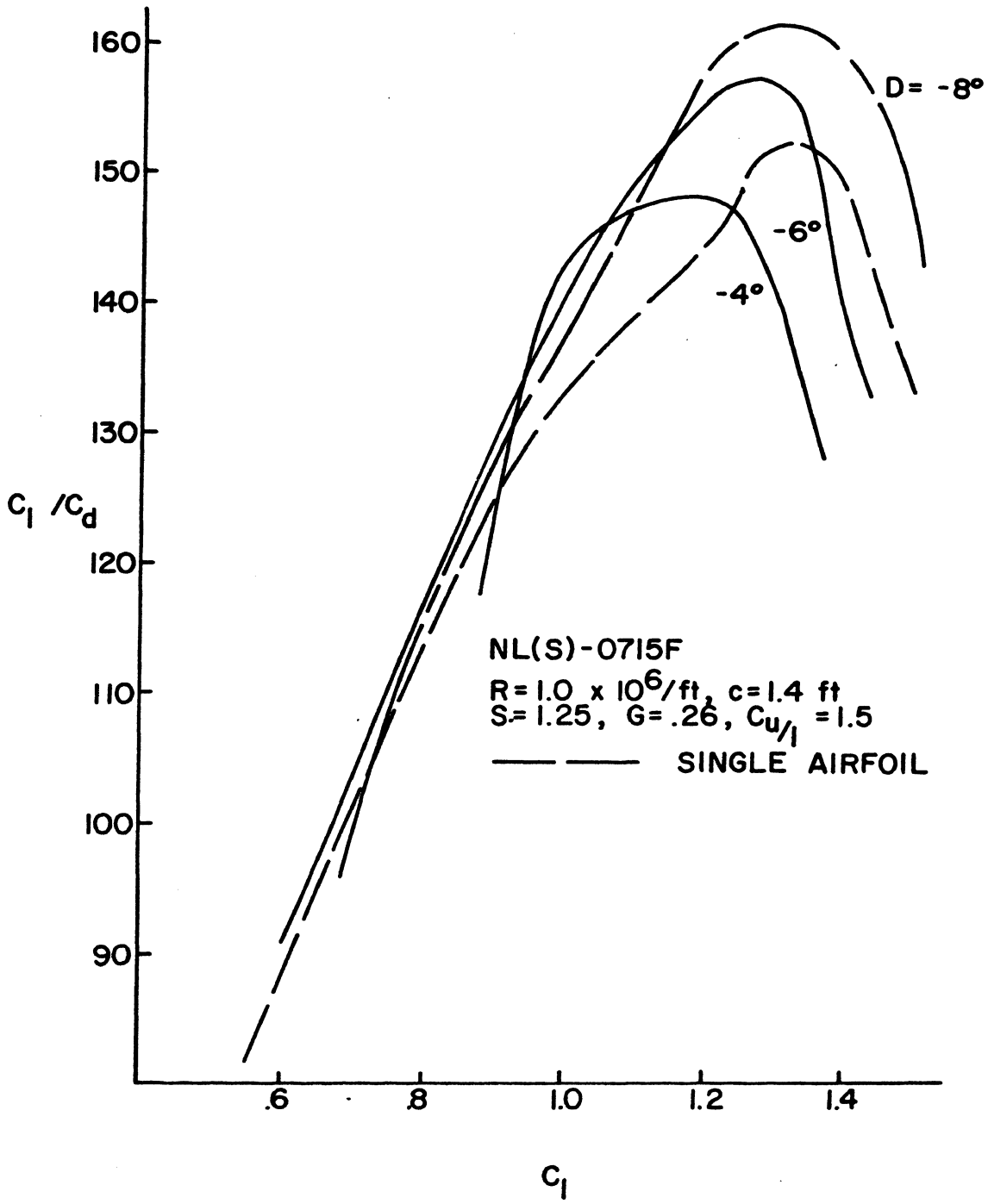

Figure 5. NL(S)-0715F Two-Dimensional Decalage Study Results for a Chord Ratio of 1.5

APPENDIX C

COMBINATIONS OF MS(1)-0313 AND NL(S)-0715F AIRFOILS

Combinations of the MS(1)-0313 and NL(S)-0715F dual airfoil results are summarized in Figures 1 through 11. The position of the airfoils: NL(S)-0715F, top and MS(1)-0313 bottom (WNM) are illustrated in Figures 1 through 5, while the MS(1)-0313, top and NL(S)-0715F, bottom (WMN) are illustrated in Figures 6 through 11. Variations in chord ratio, stagger, and decalage for the WNM system resulted in little improvement over the single NL(S)-0715F airfoil below a lift coefficient of 0.8. However, for chord ratios greater than one, illustrated in Figures 4 and 5, several of the dual airfoil systems were substantially inferior to the single NL(S)-0715F airfoil.

In general, the WMN configurations produced poor results compared to the single NL(S)-0715F airfoil, illustrated in Figures 6 through 11. For chord ratios less than one, Figures 6 through 8, neither stagger nor decalage changes obtained much advantage over the single NL(S)-0715F airfoil, below a lift coefficient of 0.7. Similarly, at chord ratios greater than one, Figures 9 through 11, there was very little improvement of the dual airfoils over the single NL(S)-0715F airfoil throughout the stagger and decalage variations.

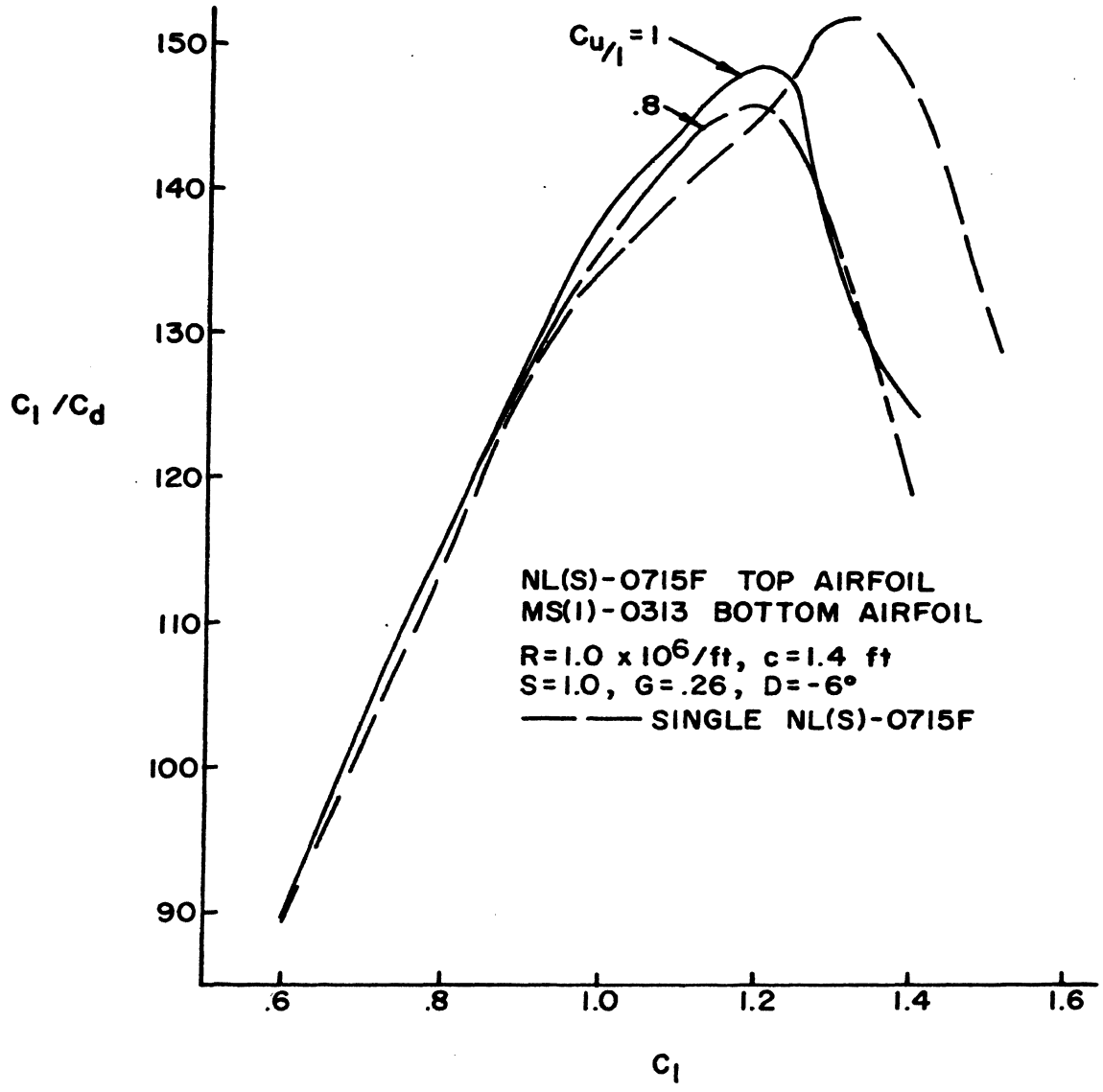

Figure 1. NL(S)-0715F and MS(1)-0313 Two-Dimensional Chord Ratio Less Than One Study Results

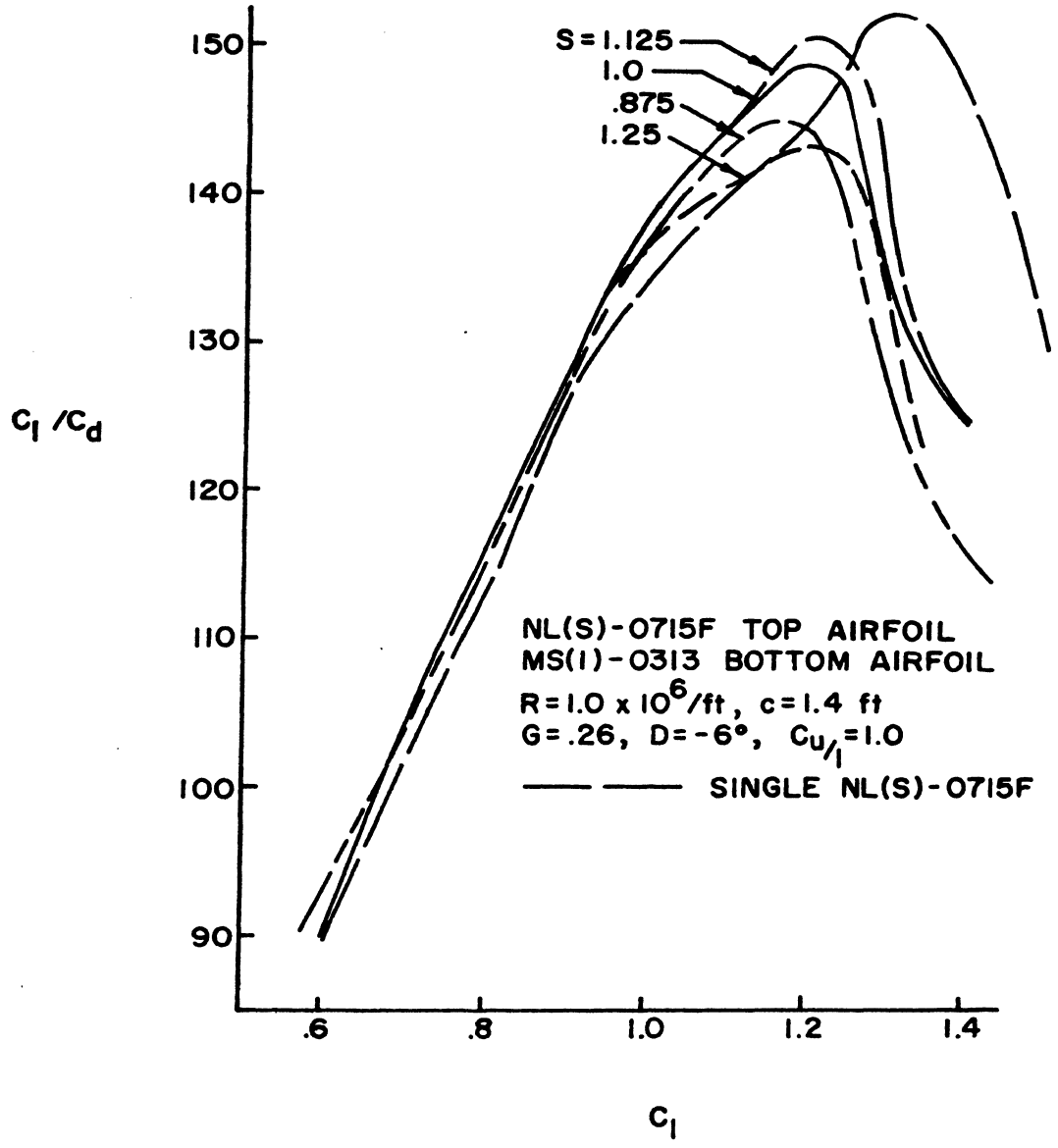

Figure 2. NL(S)-0715F and MS(1)-0313 Two-Dimensional Stagger Study Results for Chord Ratio of 1.0

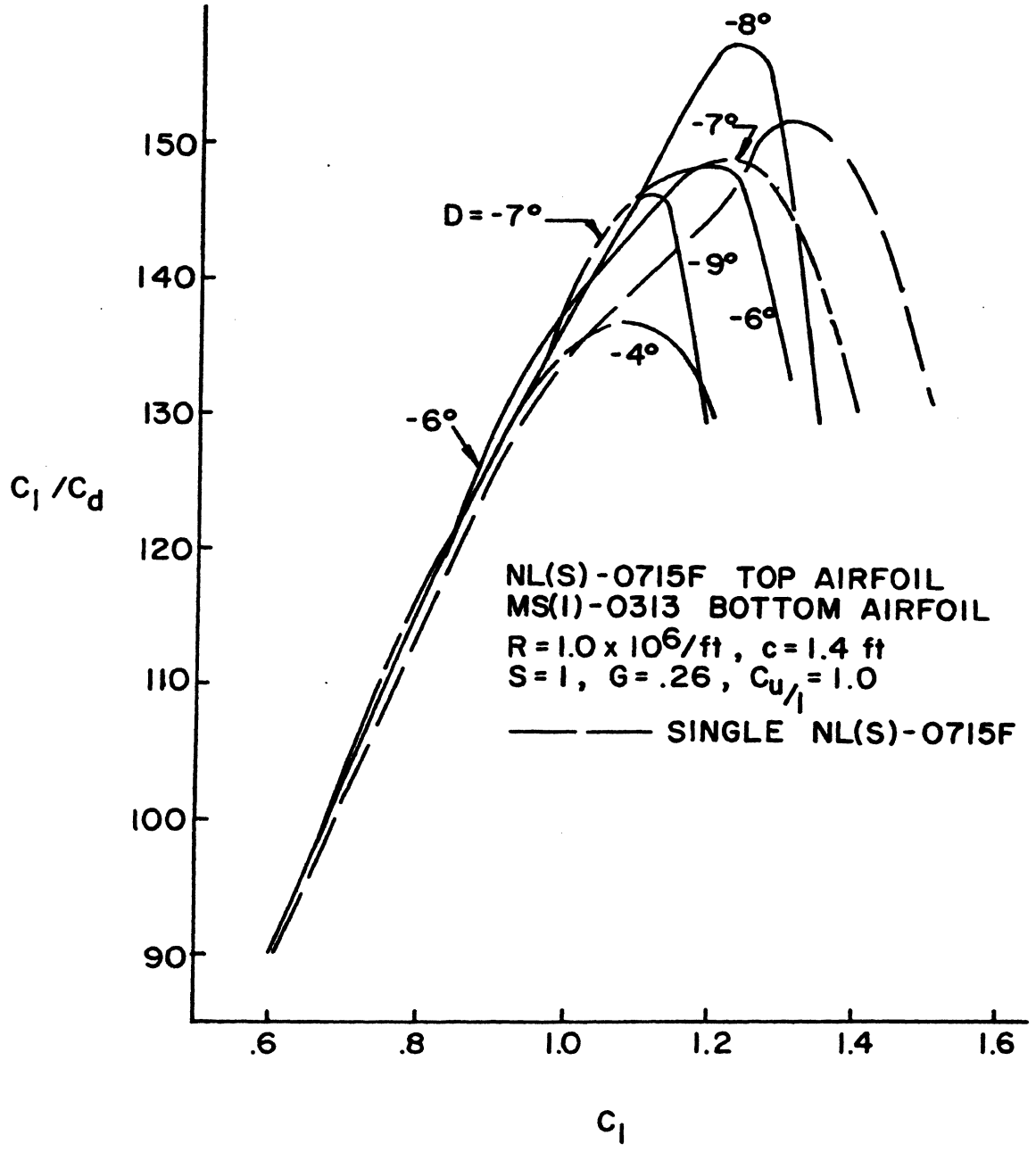

Figure 3. NL(S)-0715F and MS(1)-0313 Two-Dimensional Decalage Study Results for Chord Ratio of 1.0

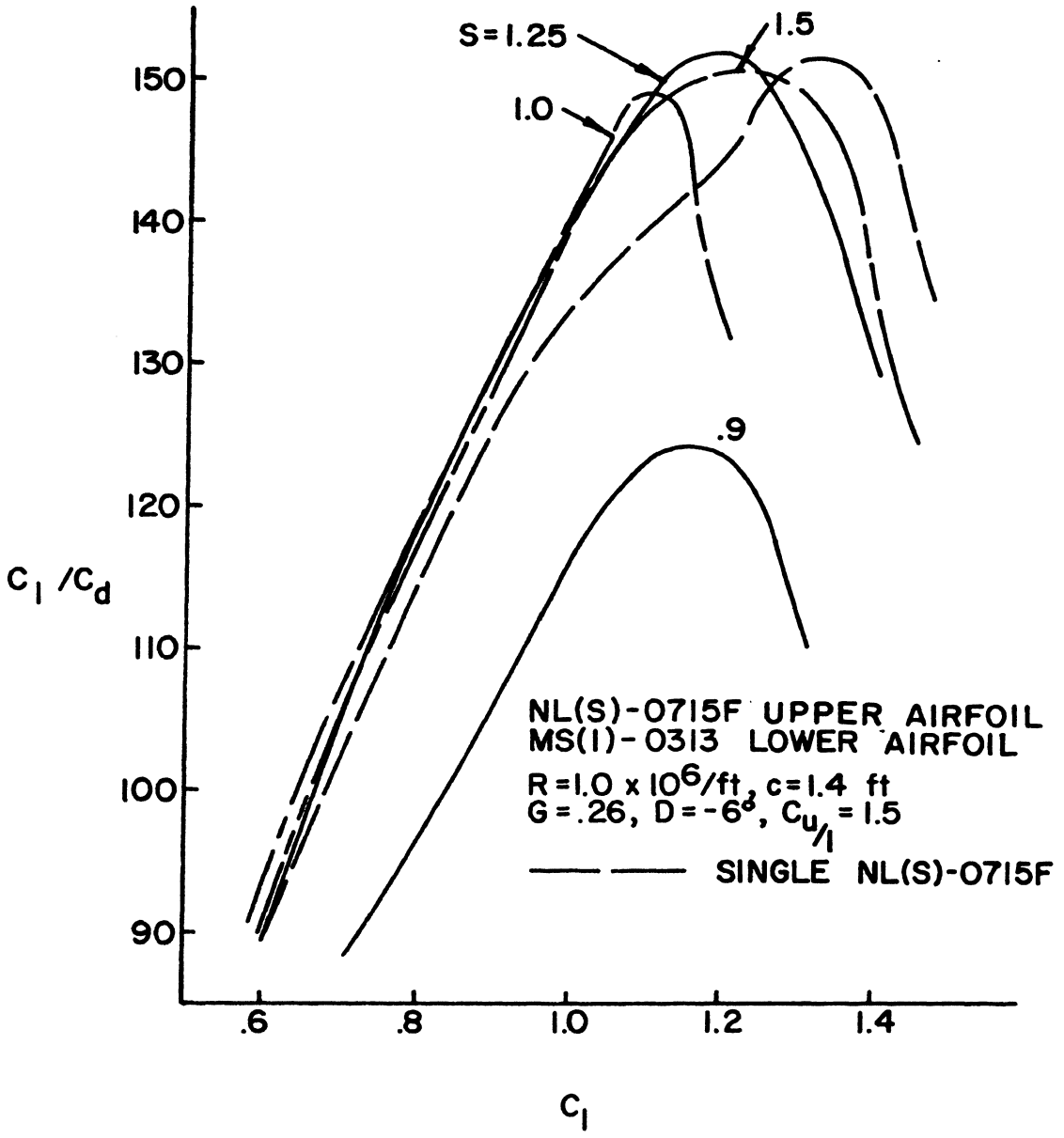

Figure 4. NL(S)-0715F and MS(1)-0313 Two-Dimensional Stagger Study Results for Chord Ratio of 1.5

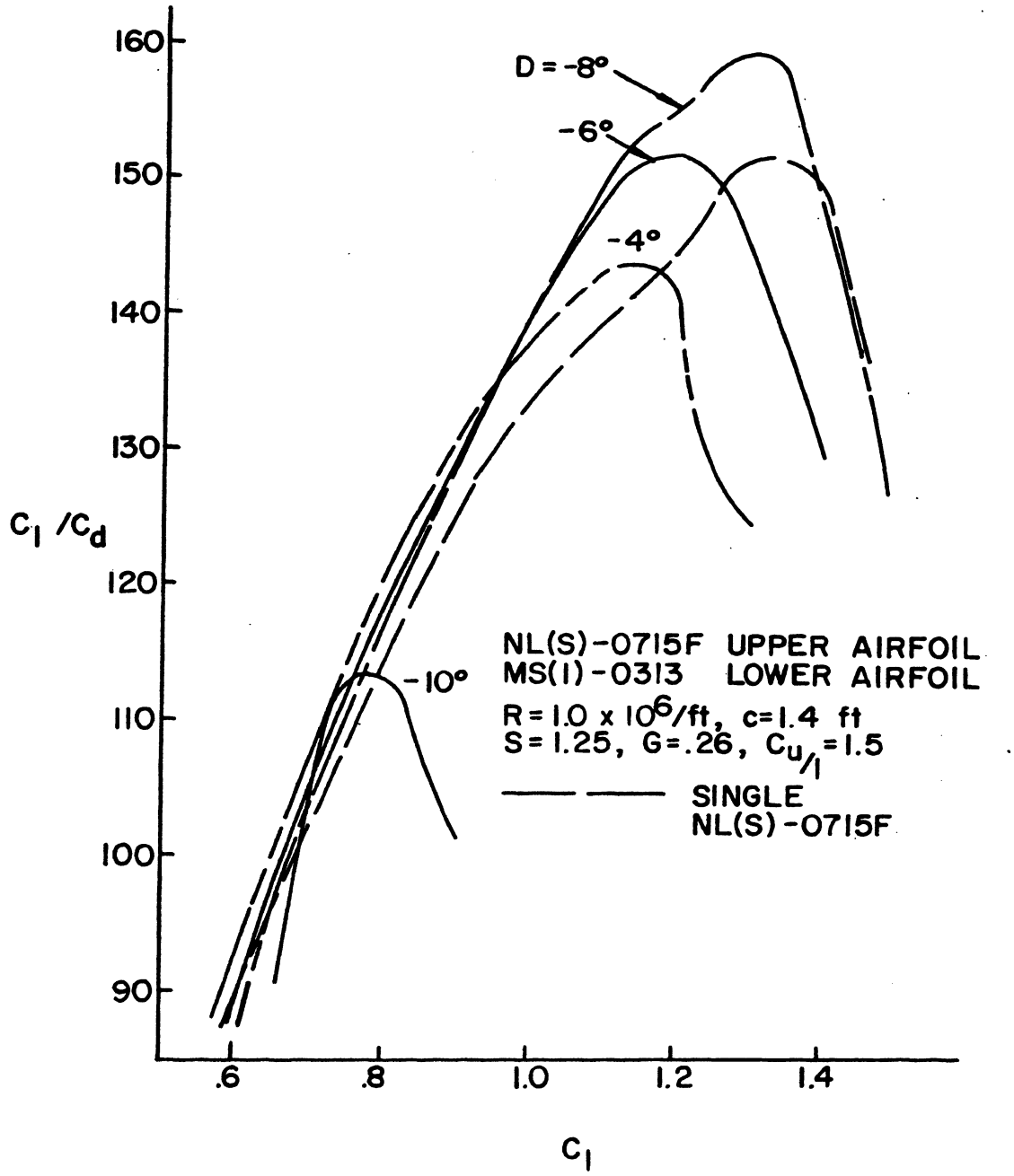

Figure 5. NL(S)-0715F and MS(1)-0313 Two-Dimensional Decalage Study Results for Chord Ratio of 1.5

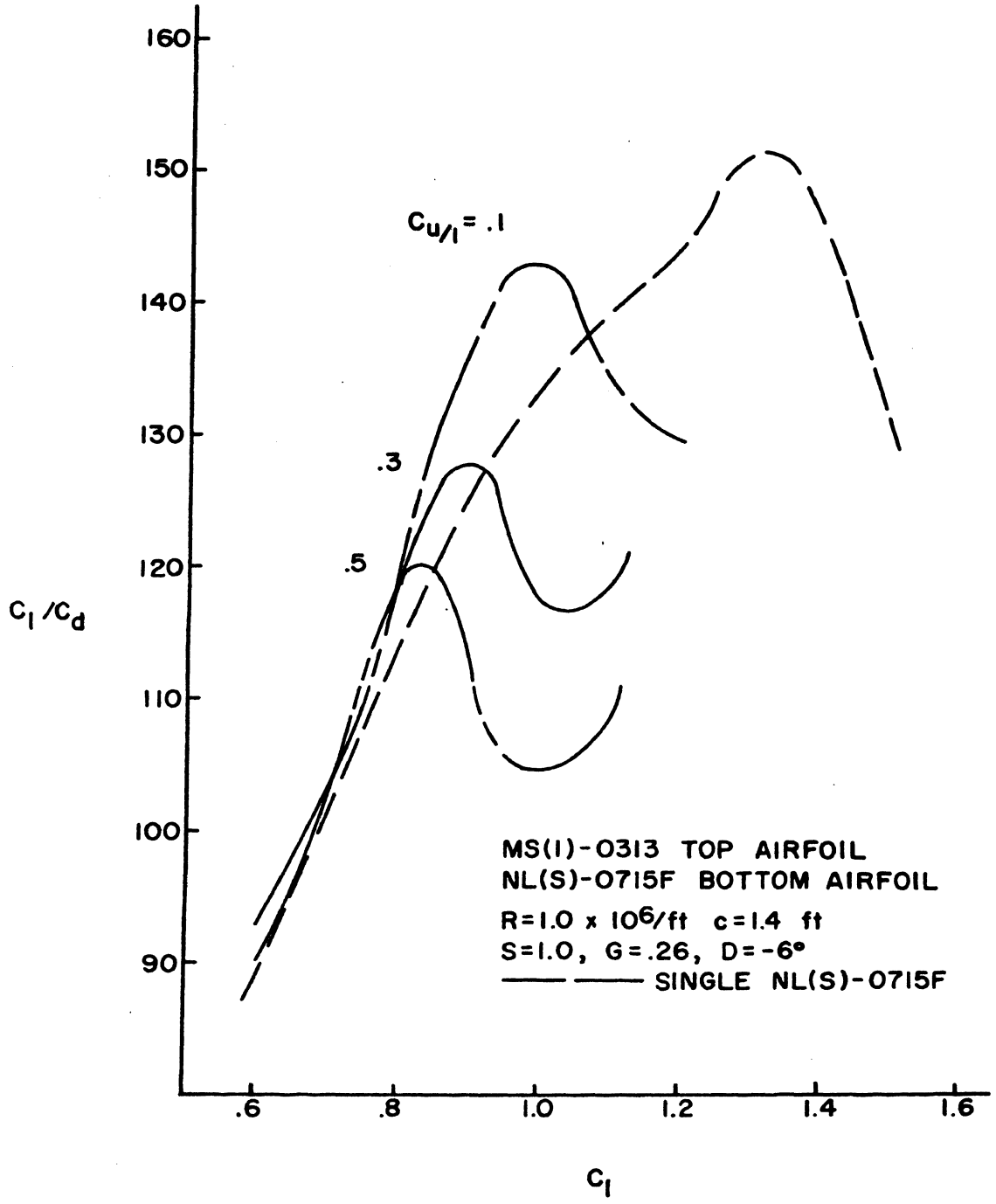

Figure 6. MS(1)-0313 and NL(S)-0715F Two-Dimensional Chord Ratio Less Than One Study Results

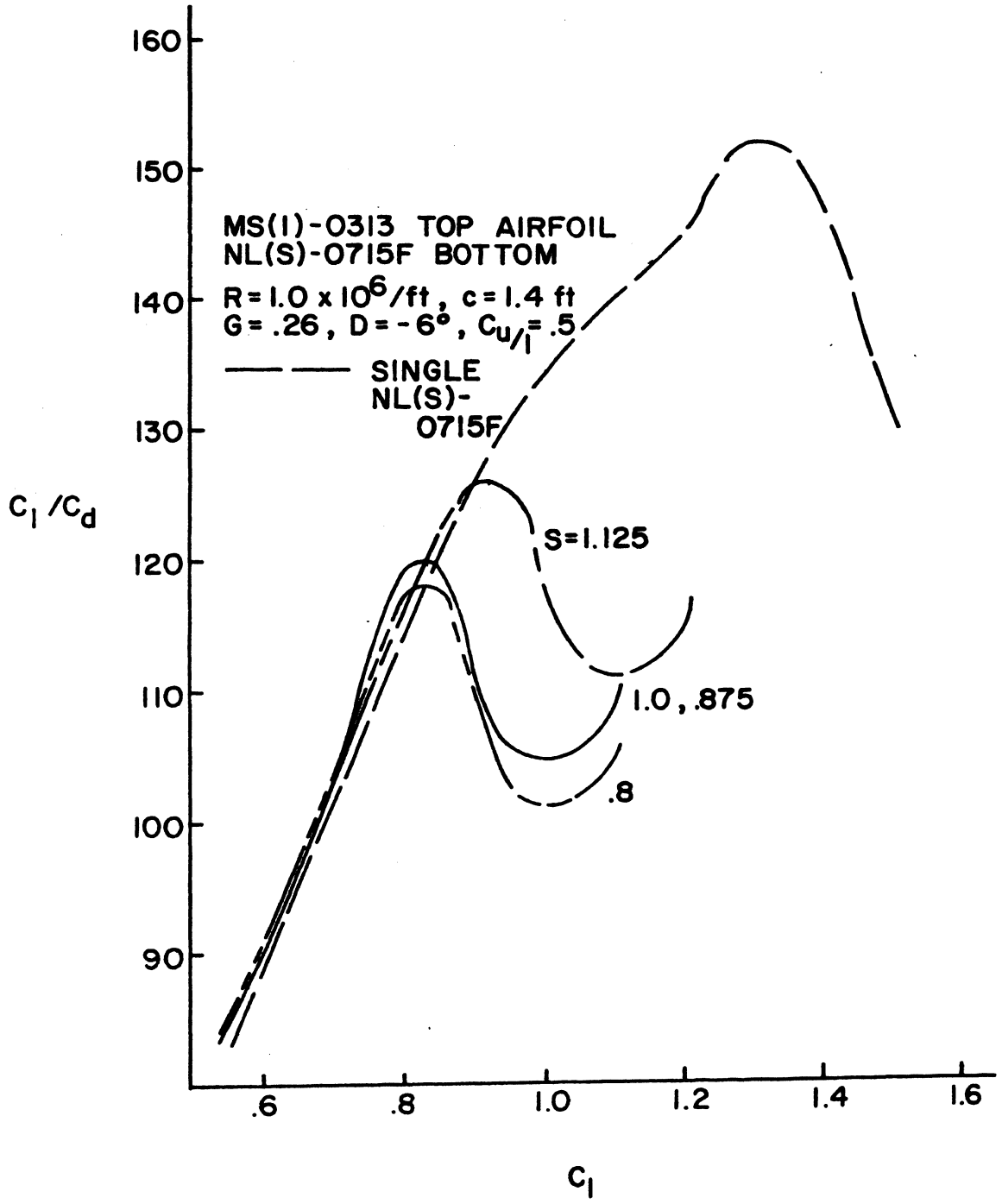

Figure 7. MS(1)-0313 and NL(S)-0715F Two-Dimensional Stagger Study Results for Chord Ratio of 0.5

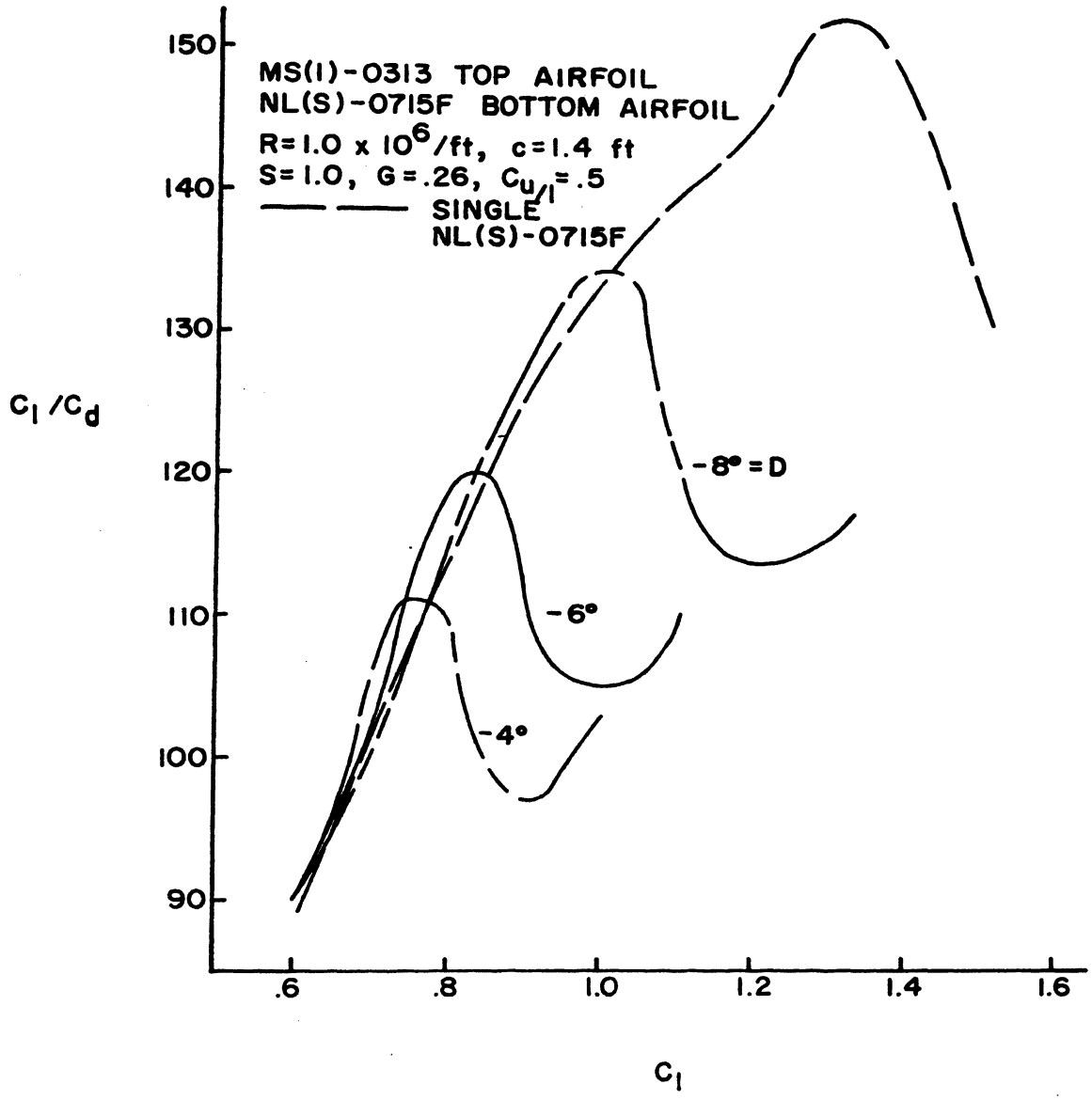

Figure 8. MS(1)-0313 and NL(S)-0715F Two-Dimensional Decalage Study Results for Chord Ratio of 0.5

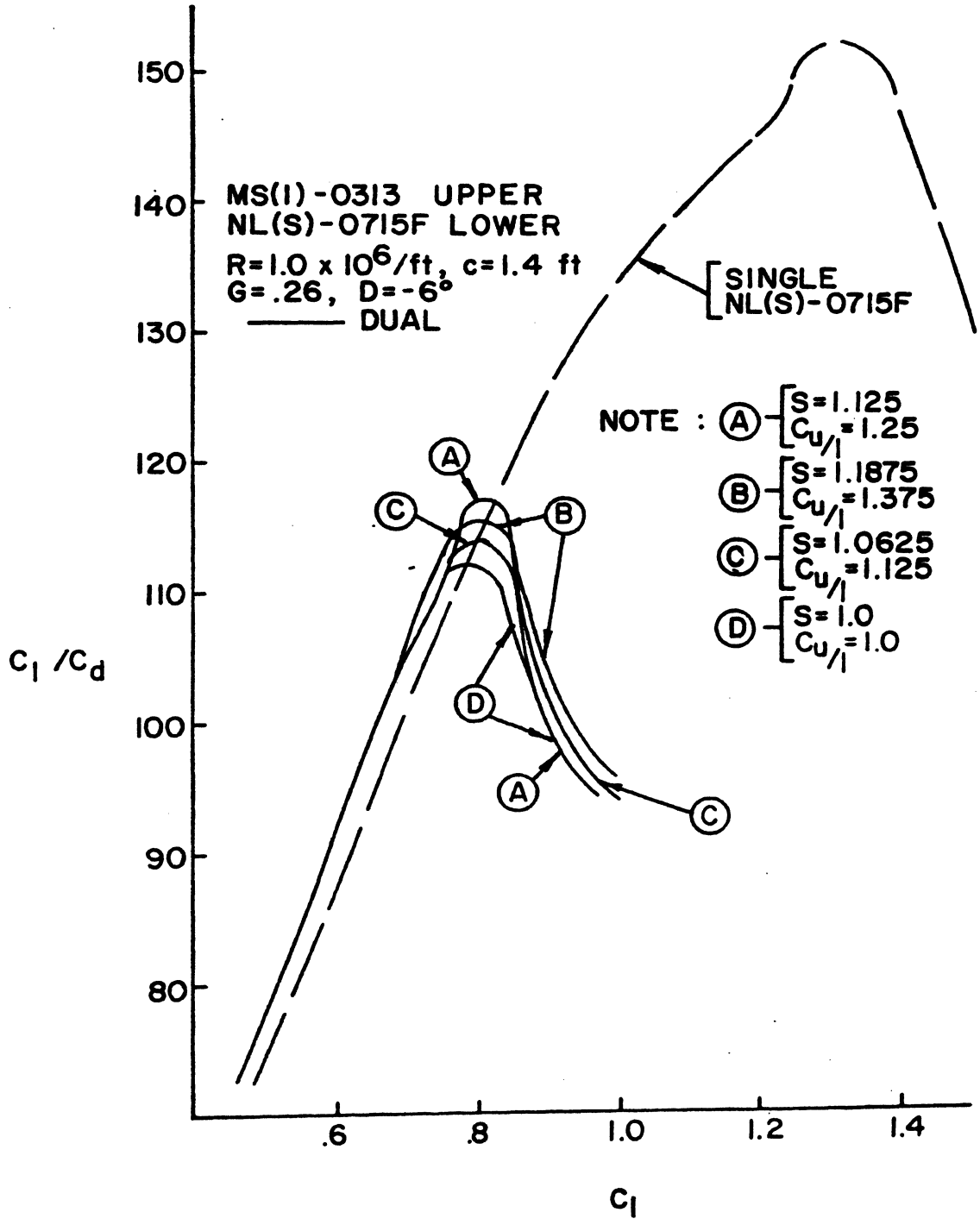

Figure 9. MS(1)-0313 and NL(S)-0715F Two-Dimensional Chord Ratio Greater Than One Study Results

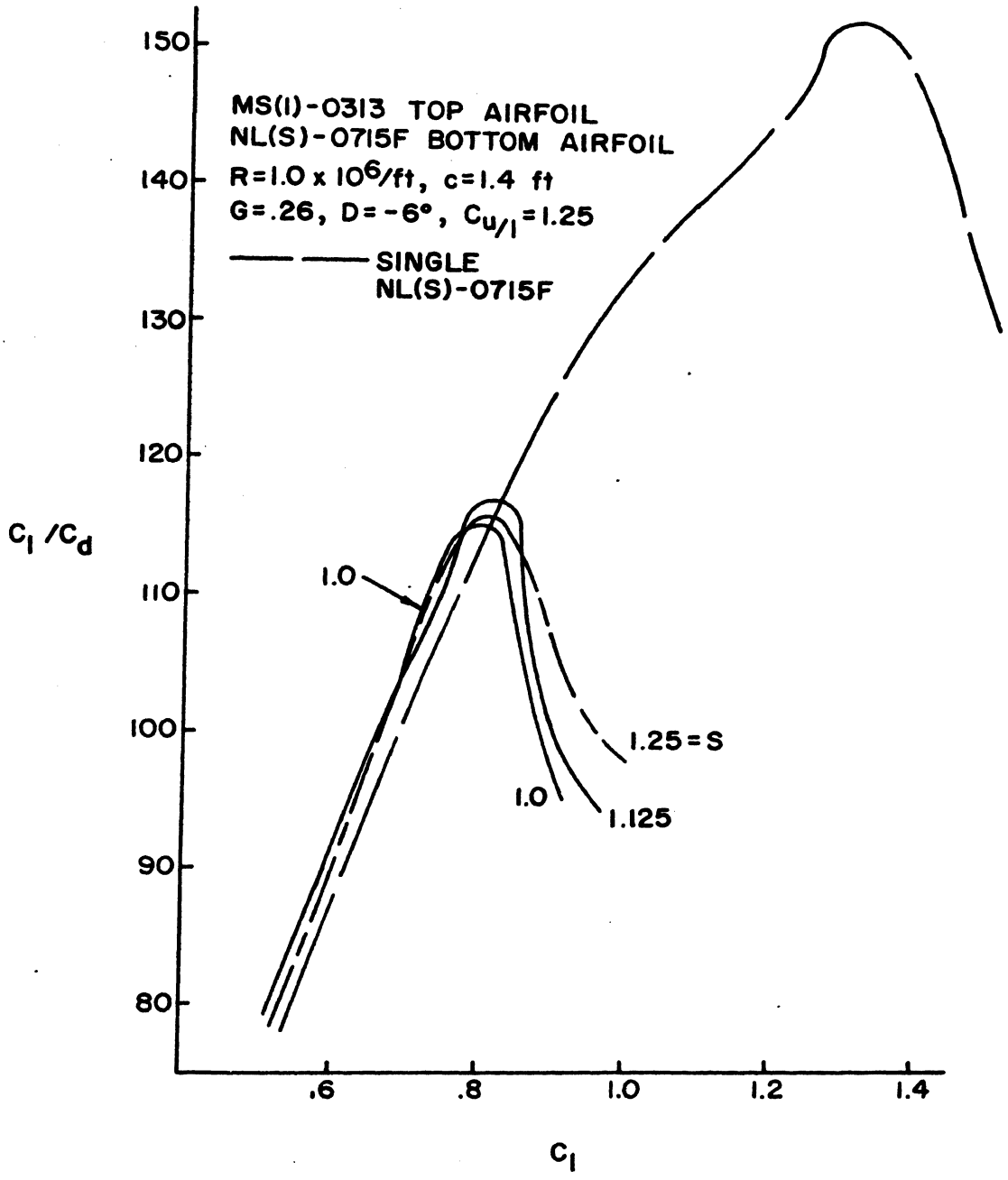

Figure 10. MS(1)-0313 and NL(S)-0715F Two-Dimensional Stagger Study Results for Chord Ratio of 1.25

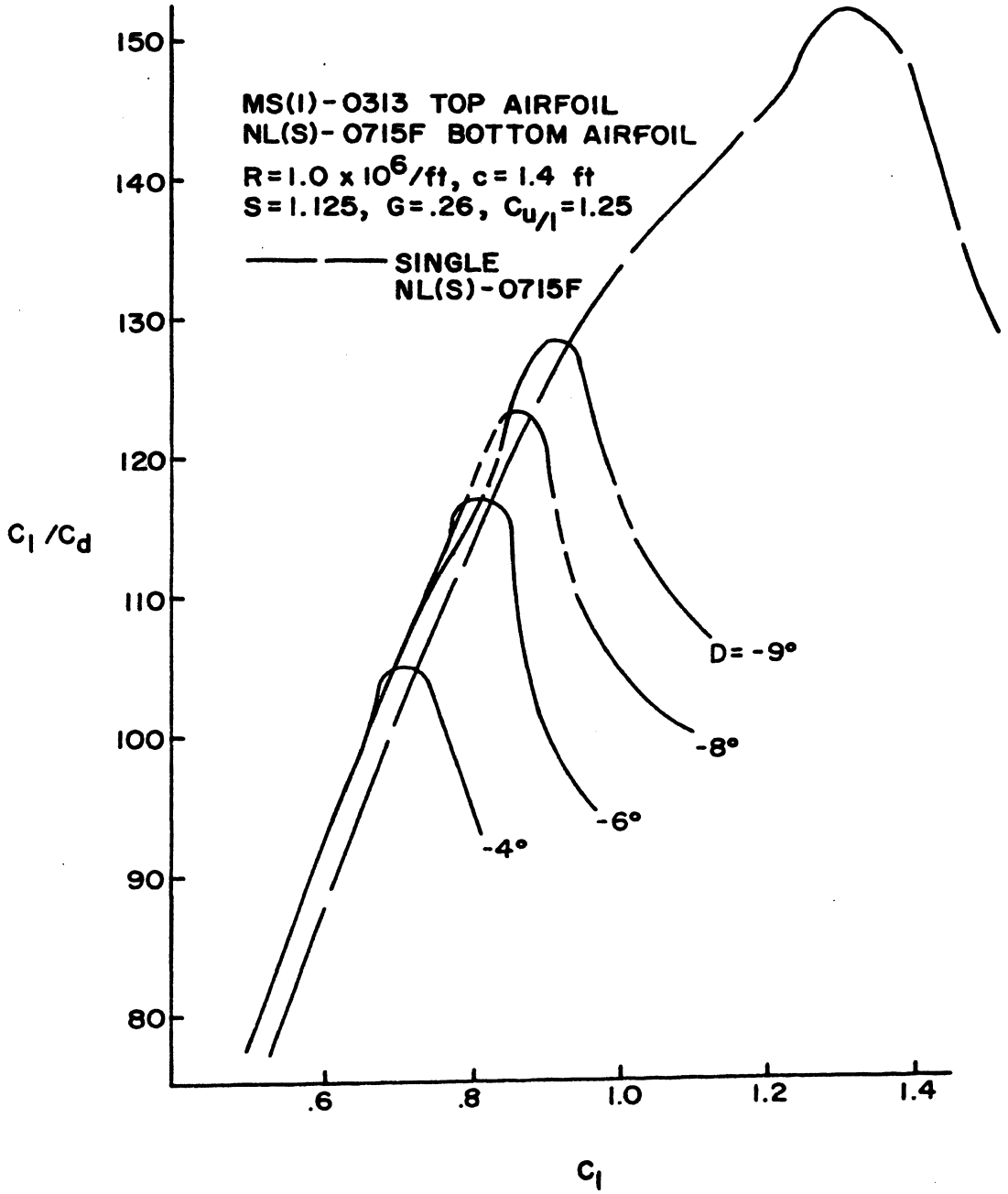

Figure 11. MS(1)-0313 and NL(S)-0715F Two-Dimensional Decalage Study Results for Chord Ratio of 1.25

APPENDIX D

FLAPPED MS(1)-0313 AIRFOIL

Combinations of the flapped and unflapped MS(1)-0313 airfoil are illustrated in Figures 1 through 4. Chord ratios 1.0 and 0.708 were used, shown in Figure 1, since the unflapped dual MS(1)-0313 airfoil peaked around these ratios. By holding the other three parameters constant, a chord ratio of 0.708 was chosen over the 1.0 ratio. The 0.708 case maintained the highest lift-to-drag ratios as compared to the single unflapped single MS(1)-0313 airfoil below a lift coefficient of 0.6. A D=-6 degrees optimized over the other angles shown in Figure 2. No stagger studies were performed for the flapped dual airfoil systems since the MS(1)-0313 airfoil at both chord ratios, 1.0 and 0.708, optimized at S=1.

The dual MS(1)-0313 airfoils with the lower airfoil flapped and chord ratio of one optimized above the single unflapped airfoil in Figure 3. The chord ratio of 0.708 results at a constant S=1, G=0.26, and D=-6 degrees fell below the single airfoil. Therefore, a decalage study was performed using only the dual airfoil of equal chords. D=-8 degrees peaked above the other angles in Figure 4. The D=-8 degrees was chosen for farther study since it also remained relatively equivalent to the D=-6 degrees case at lower lift coefficients.

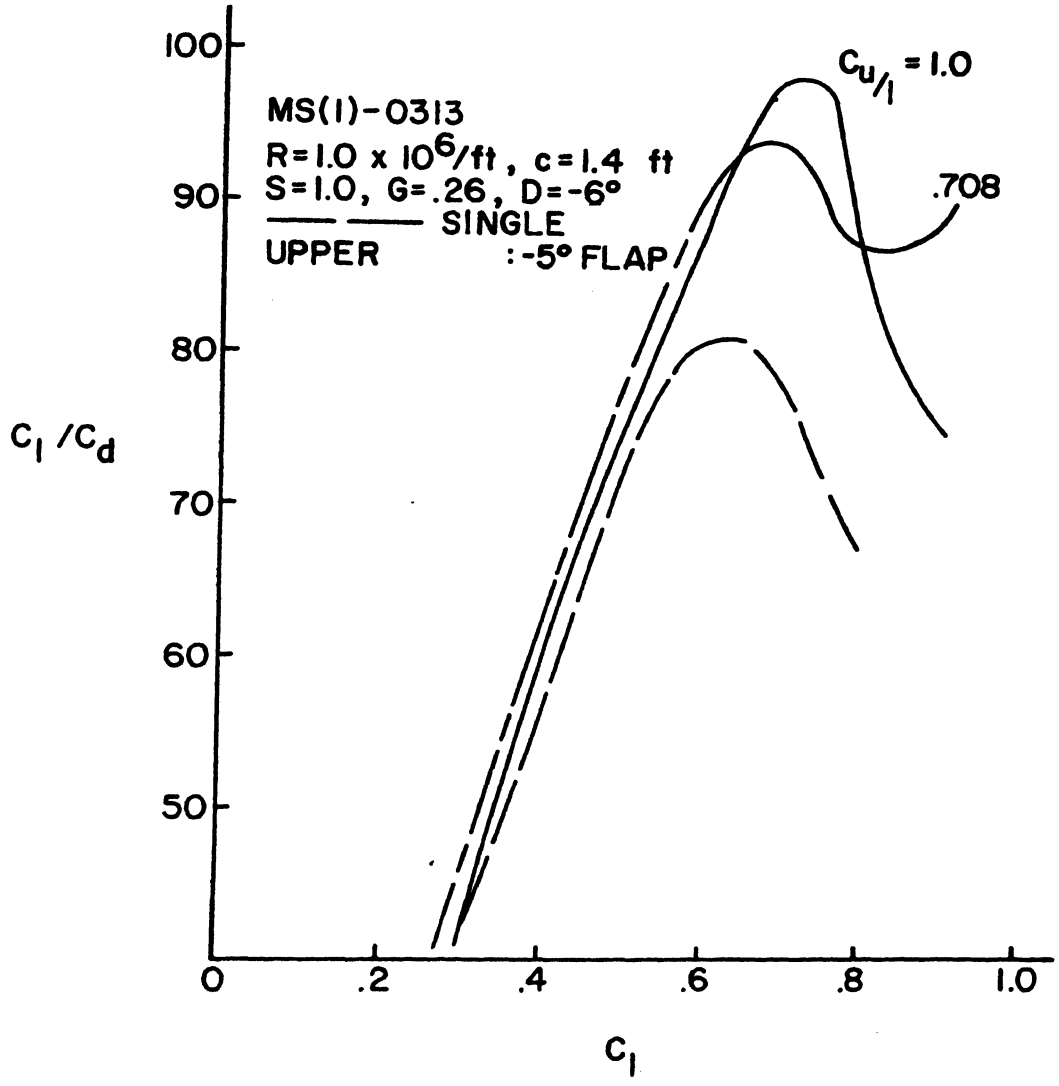

Figure 1. Upper Flapped MS(1)-0313 Two-Dimensional Chord Ratio Study Results

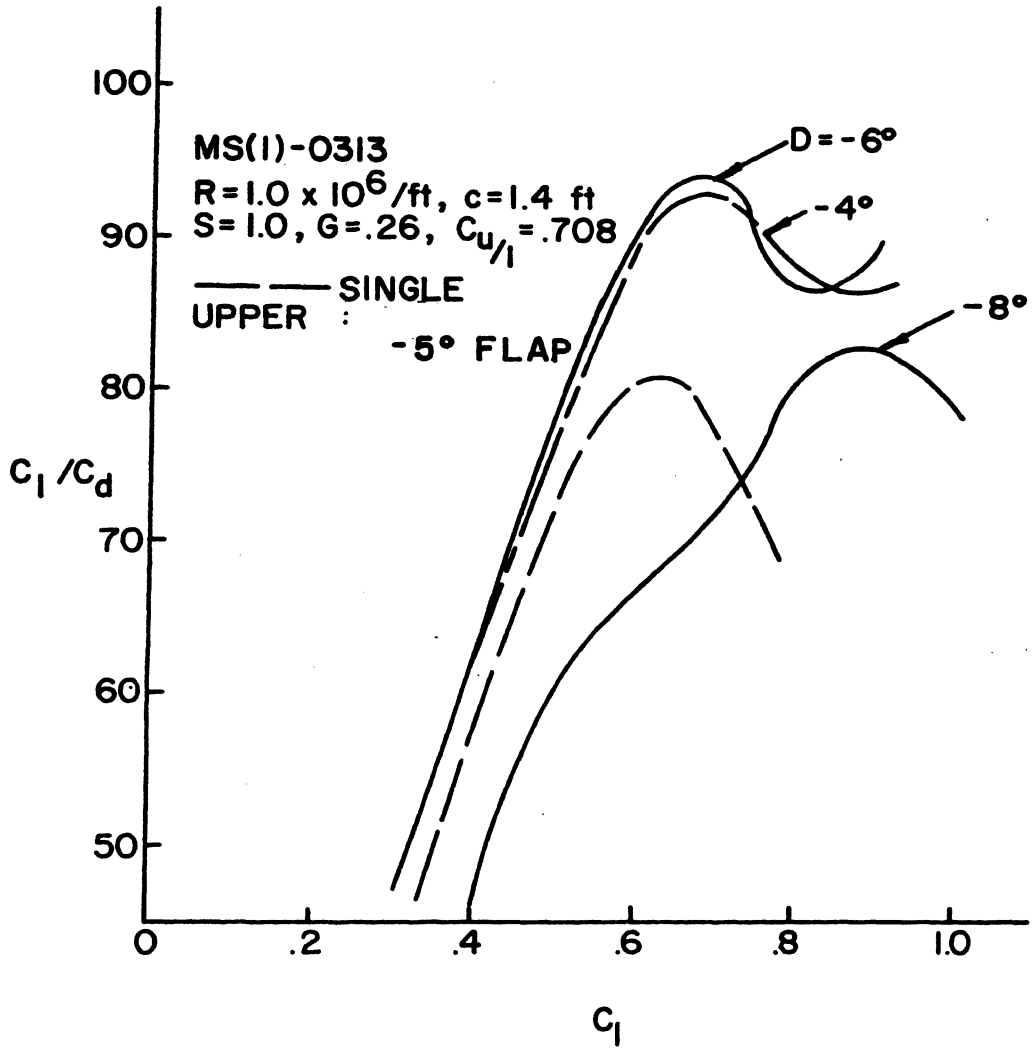

Figure 2. Upper Flapped MS(1)-0313 Two-Dimensional Decalage Study Results for Chord Ratio of 0.708

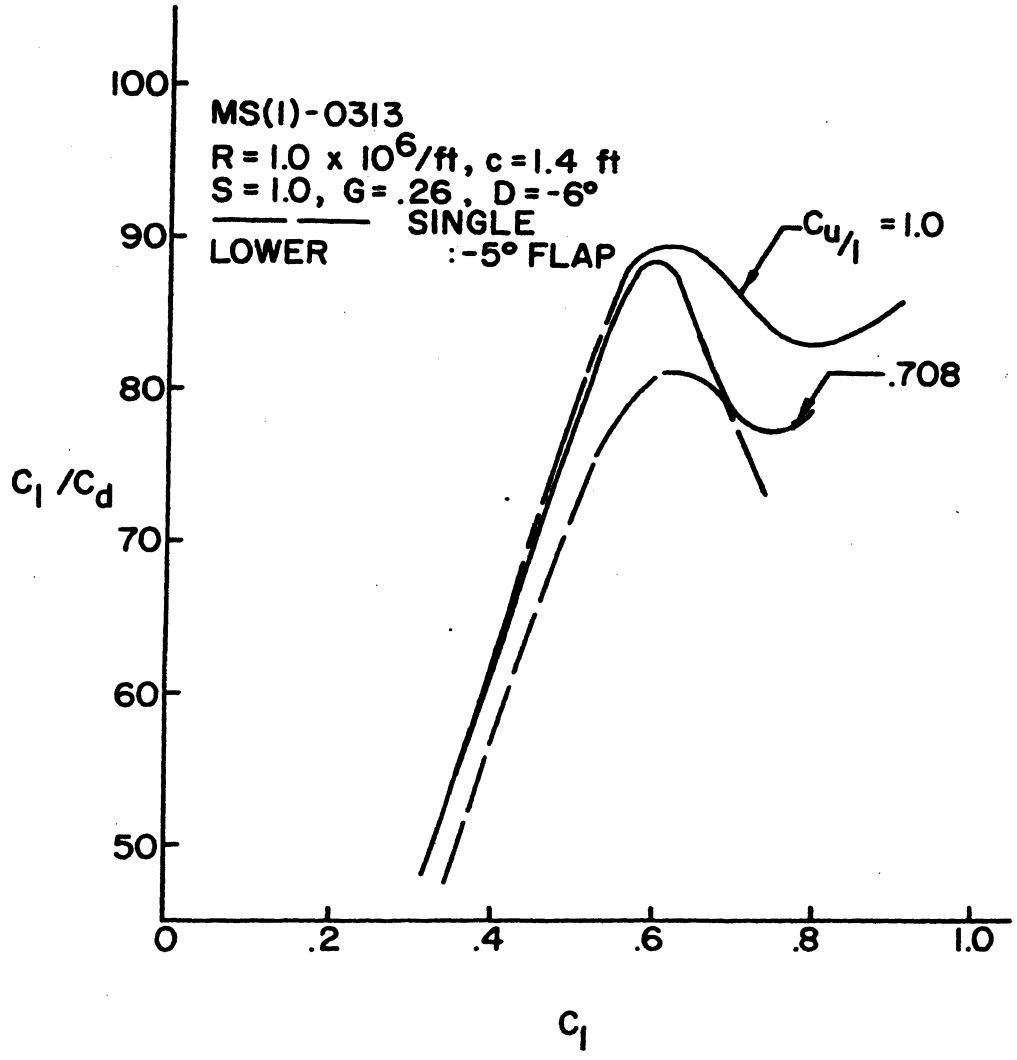

Figure 3. Lower Flapped MS(1)-0313 Two-Dimensional Chord Ratio Study Results

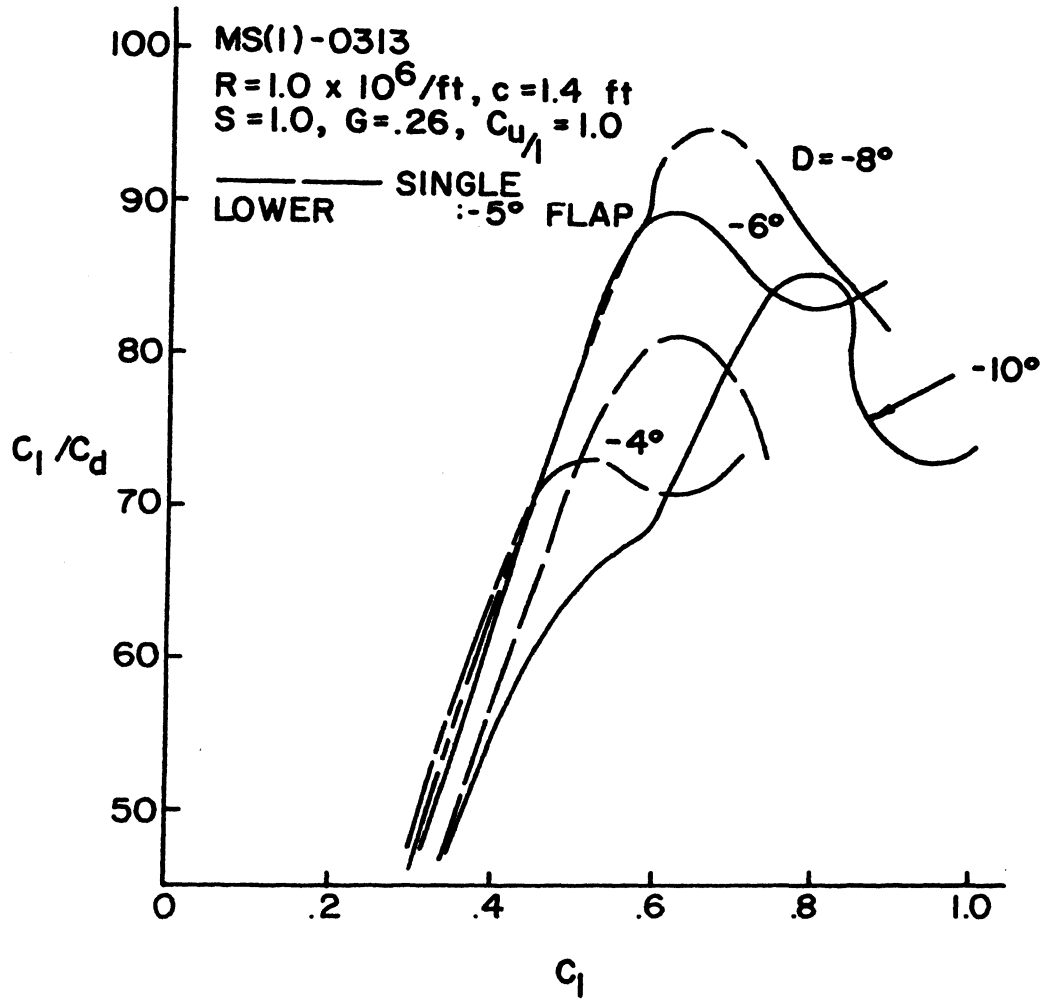

Figure 4. Lower Flapped MS(1)-0313 Two-Dimensional Decalage Study Results for Chord Ratio of 1.0

APPENDIX E

RONCZ AIRFOILS

Figures 1 and 2 show the results of the parametric study for the RONCZ 1073 and 1085 airfoil sections. In Figure 1, RONCZ 1073 at a chord ratio of 1.0 and 0.708 was compared to the single RONCZ 1073 airfoil while holding S=1, G=0.26, and D=-6 degree constant. Both dual airfoils obtained very little drag reduction over their single airfoil counterparts, that is a single airfoil producing the equivalent lift as a dual airfoil combination, below a lift coefficient of 0.9. Since there were no substantial improvements for the RONCZ 1073 dual airfoil over its single airfoil counterpart, no farther studies were performed using this airfoil.

The equal chord ratio for the RONCZ 1085 dual airfoils possessed the highest lift-to-drag ratios for all the lift coefficients shown. Therefore, a decalage study was performed summarized in Figure 2. D=-8 degrees peaked above the other cases around a lift coefficient of 0.9. However, at the 0.65 lift coefficient the single airfoil exhibited slightly better performance over the D=-8 degree case. Similarly, below the lift coefficient of 0.8, the effect of decalage was negligible for improving the dual airfoils over the single airfoil counterparts. For these reasons, no further parametric studies were performed using the RONCZ 1085 airfoil.

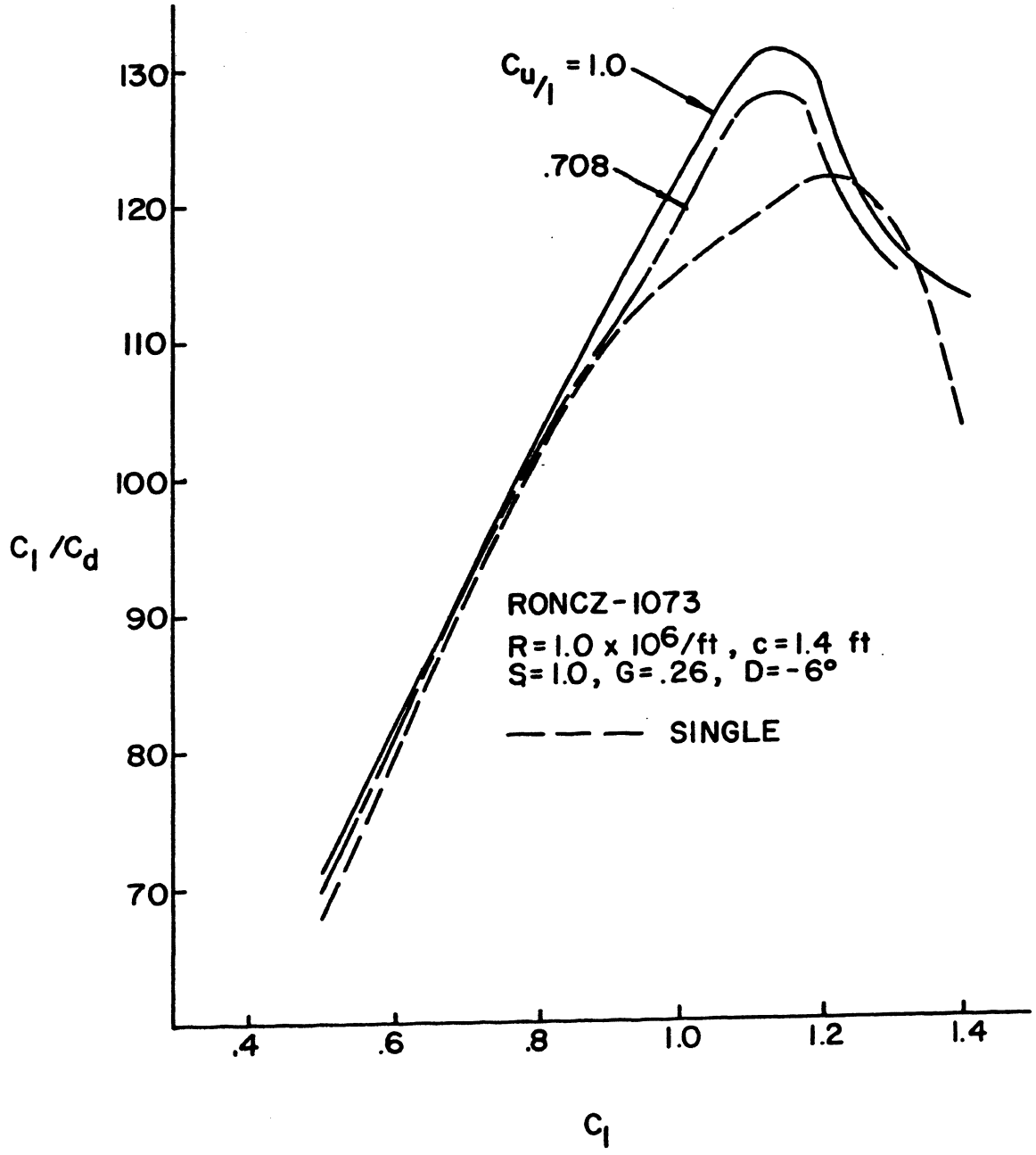

Figure 1. RONCZ 1073 Two-Dimensional Chord Ratio Study Results

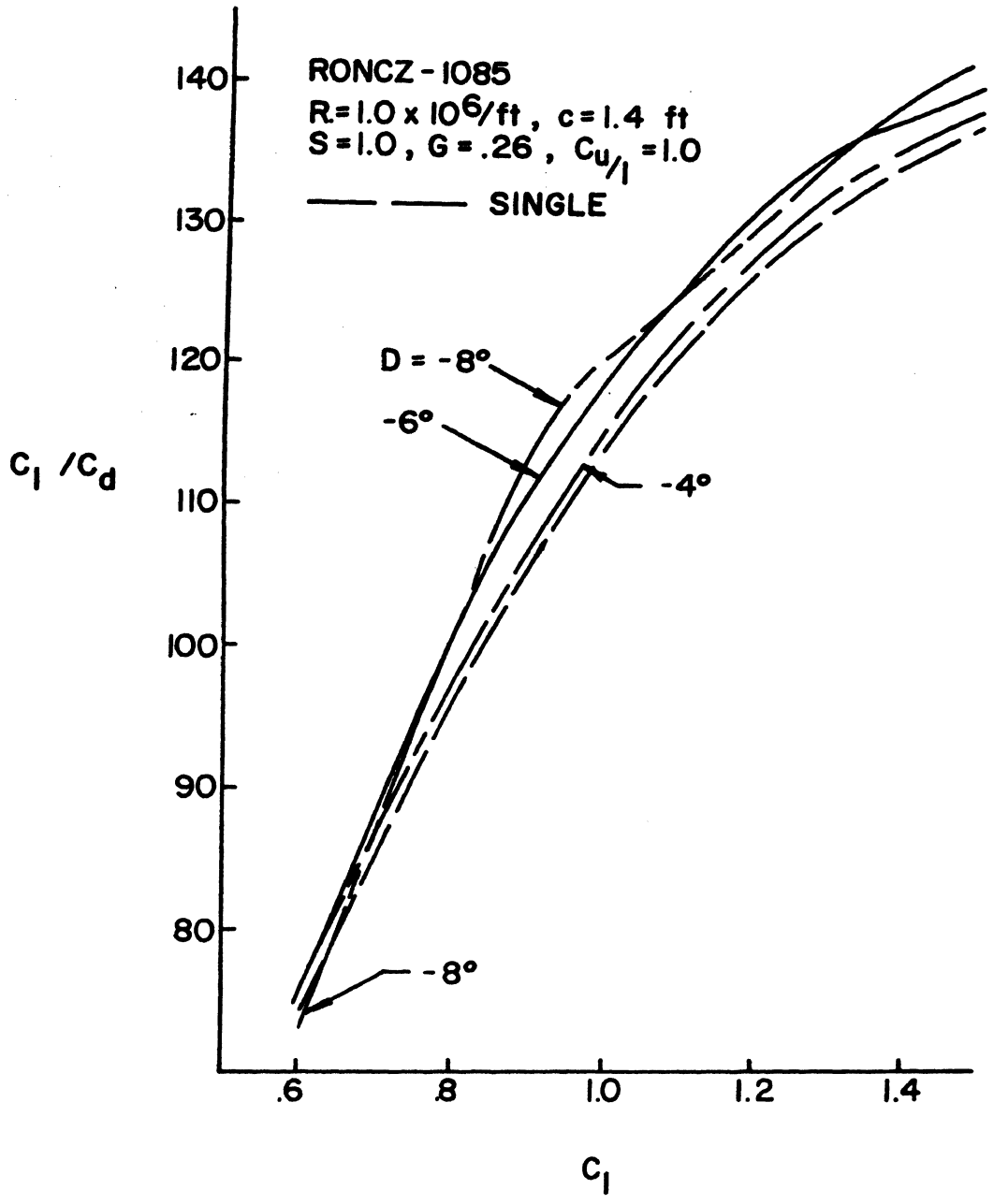

Figure 2. RONCZ 1085 Two-Dimensional Decalage Study Results for Chord Ratio of 1.0

APPENDIX F

0.708 DUAL WING AIRCRAFT

TABLE I. 0.708 DUAL WING AIRCRAFT GEOMETRIC CHARACTERISTICS

	MS(1)-0313	
	6-PLACE	12-PLACE
Overall Geometry		
Length (ft)	26.4	41.6
Span (ft)	39.9	57.1
Height (ft)	11.3	14.2
Reference area (ft^2)	93.0	192.4
c.g. range (aft of nose in ft)	12.60-13.52	20.07-21.60
a.c. (aft of nose in ft)	13.62	21.78
Wing		
Area (ft^2)	93.0	192.4
Span (ft)	38.6	55.5
Mean aerodynamic chord (ft)	2.46	3.54
Aspect Ratio	16	16
Dihedral (deg)	3	3

TABLE I. (Continued)

	MS(1)-0313	
	6-PLACE	12-PLACE
Thickness-to-chord ratio	13%	13%
Taper ratio	0.6	0.6
a.c. (aft of nose in ft)	11.78	18.89
Horizontal Tail		
Area (ft^2)	30	55
Span (ft)	12	14.8
Aspect ratio	4.8	4.0
Taper ratio	0.5	0.8
Vertical Tail		
Area (ft^2) upper/lower	16.3/8.8	40
Span (ft) upper/lower	5.0/3.5	8.4
Aspect ratio upper/lower	1.5/1.4	1.8
Taper ratio upper/lower	0.4/0.3	0.3

TABLE I. (Continued)

	MS(1)-0313	
	6-PLACE	12-PLACE
Fuselage		
Maximum width (exterior) (in)	48	68
Maximum height (exterior) (in)	56	68
Length (ft)	25	40
Cabin width (in)	44	64
Cabin height (in)	50	60
Cabin length (ft)	14.5	24.2
Propeller		
Propeller diameter (ft)	7.5	